Received: 8 March 2024 | Revised: 31 May 2024 | Accepted: 22 July 2024

DOI: 10.1111/mec.17487

ORIGINAL ARTICLE

MOLECULAR ECOLOGY WILEY

Genomic, morphological and physiological data support fast ecotypic differentiation and incipient speciation in an alpine diving beetle

Susana Pallarés[1] | Joaquín Ortego[2] | José Antonio Carbonell[1] | Eduardo Franco-Fuentes[1] | David T. Bilton[3,4] | Andrés Millán[5] | Pedro Abellán[1]

[1]Department of Zoology, University of Seville, Seville, Spain

[2]Department of Ecology and Evolution, Estación Biológica de Doñana, EBD-CSIC, Seville, Spain

[3]School of Biological and Marine Sciences, University of Plymouth, Plymouth, UK

[4]Department of Zoology, University of Johannesburg, Johannesburg, South Africa

[5]Department of Ecology and Hydrology, University of Murcia, Murcia, Spain

Correspondence
Susana Pallarés, Department of Ecology and Hydrology, University of Murcia, Murcia, Spain.
Email: susana.pallares@um.es

Present address
José Antonio Carbonell, Department of Zoology, University of Murcia, Cordoba, Spain

Funding information
Next Generation EU; Ministerio de Ciencia e Innovación, Grant/Award Number: PID2019-108895GB-I00; Ministerio de Universidades, Grant/Award Number: 19868; Consejería de Economía, Conocimiento, Empresas y Universidad, Junta de Andalucía, Grant/Award Number: SP-DOC_01211

Handling Editor: Brent Emerson

Abstract

An intricate interplay between evolutionary and demographic processes has frequently resulted in complex patterns of genetic and phenotypic diversity in alpine lineages, posing serious challenges to species delimitation and biodiversity conservation planning. Here we integrate genomic data, geometric morphometric analyses and thermal tolerance experiments to explore the role of Pleistocene climatic changes and adaptation to alpine environments on patterns of genomic and phenotypic variation in diving beetles from the taxonomically complex *Agabus bipustulatus* species group. Genetic structure and phylogenomic analyses revealed the presence of three geographically cohesive lineages, two representing trans-Palearctic and Iberian populations of the elevation-generalist *A. bipustulatus* and another corresponding to the strictly-alpine *A. nevadensis*, a narrow-range endemic taxon from the Sierra Nevada mountain range in southeastern Iberia. The best-supported model of lineage divergence, along with the existence of pervasive genetic introgression and admixture in secondary contact zones, is consistent with a scenario of population isolation and connectivity linked to Quaternary climatic oscillations. Our results suggest that *A. nevadensis* is an alpine ecotype of *A. bipustulatus*, whose genotypic, morphological and physiological differentiation likely resulted from an interplay between population isolation and local altitudinal adaptation. Remarkably, within the Iberian Peninsula, such ecotypic differentiation is unique to Sierra Nevada populations and has not been replicated in other alpine populations of *A. bipustulatus*. Collectively, our study supports fast ecotypic differentiation and incipient speciation processes within the study complex and points to Pleistocene glaciations and local adaptation along elevational gradients as key drivers of biodiversity generation in alpine environments.

KEYWORDS
alpine ecosystems, Coleoptera, glacial refugia, hybridisation, integrative taxonomy, Pleistocene speciation, sky-islands

1 | INTRODUCTION

Understanding the processes that generate and maintain biodiversity is a central issue in evolutionary biology (Avise, 2000), with clear implications for conservation management (Coates et al., 2018; Seehausen, 2006; Stanton et al., 2019). High-elevation temperate mountains, traditionally considered as centres of lineage diversification or 'species pumps' (Schoville et al., 2012), provide a global model for understanding patterns of biodiversity and the evolutionary processes involved in speciation (Antonelli et al., 2018; Flantua et al., 2020).

Historical environmental changes during repeated glaciation and deglaciation events in the Pleistocene had a dramatic impact on the patterns of ecological and genetic diversity of both alpine and lowland biotas (Baker, 2008; Hewitt, 2000; Weir & Schluter, 2004). Glacial cycles have induced range expansions during either glacial or interglacial periods – depending on the ecology of the species – followed by range contractions to refugia when conditions became more adverse (Bennett & Provan, 2008; Dynesius & Jansson, 2000; Stewart et al., 2010). Pleistocene ice ages have often promoted lineage diversification via cycles of allopatry in ecologically divergent refugia, which has been identified as an important driver of the formation of alpine endemics (Tribsch, 2004). Such alpine endemics are subject to repeated cycles of isolation, divergent adaptation and secondary contact (e.g. the 'glacial pulse' model of alpine diversification; Maier et al., 2019). Secondary contact can accelerate speciation via the reinforcement of incipient reproductive isolation (Butlin, 1987; Hedrick, 2013) or lead to the formation of hybrid species (Mavárez & Linares, 2008; Noguerales & Ortego, 2022). However, speciation is not always a linear, unidirectional process and divergence may also slow down or even be reversed if lineages that have not evolved reproductive barriers merge when they came into secondary contact (i.e. 'speciation reversal' or 'lineage fusion'; Garrick et al., 2014; Kearns et al., 2018; Seehausen et al., 2008).

In mountain systems, lineage formation associated with glacial cycles can be accompanied by either phenotypic plasticity or local adaptation processes along altitudinal gradients, as these systems are characterised by steep environmental changes over short geographical distances (i.e. strong selection differentials; Körner, 2007; Steinbauer et al., 2013). In fact, there are numerous cases of montane and alpine forms within species and species complexes for which local adaptation and phenotypic plasticity play contrasting roles (Keller et al., 2013; Stanbrook et al., 2021; Tsuchiya et al., 2012). These lineages often show complex patterns of genetic, ecological and phenotypic diversity, prompting intense taxonomic debates (e.g. Drotz et al., 2012; McCulloch et al., 2019; Ortego et al., 2021; Tonzo et al., 2019), whose solution will require fully integrated research approaches.

The Sierra Nevada massif in southeastern Iberia is recognised as a biodiversity and endemicity hotspot for plants (Médail & Quézel, 1997, 1999) and animals (Ruano et al., 2013). Its isolation from other comparable mountain ranges (e.g. the Pyrenees) and its location at the southernmost limit of influence of Quaternary glaciations in Europe, have resulted in a high number of evolutionarily unique taxa and species assemblages in this mountain range (Zamora & Oliva, 2022). The Sierra Nevada was covered with glaciers only at elevations >2500 m, with large areas remaining free of glacial ice (Gómez-Ortiz et al., 2013). This, coupled with the large and rapid altitudinal gradient (0–3479 m in 35 km, from the coast to the highest peak), means that many taxa likely survived glacial cycles locally. As a consequence, this system provides a unique opportunity to understand processes of local adaptation linked to glacial cycles, study how species and populations have evolved in high-altitude environments and evaluate the potential impacts of ongoing climate warming on the conservation of narrowly endemic taxa.

The Sierra Nevada hosts a system of glacial ponds and lakes between approximately 2800 and 3100 m that harbour highly specific assemblages of cold-adapted macroinvertebrates, some of them microendemic to this area (Millán et al., 2013), including the diving beetle *Agabus nevadensis* Lindberg, 1939. Despite being currently recognised as a valid species (Nilsson & Hájek, 2021), its precise taxonomic status in relation to its widespread Western Palearctic congener *A. bipustulatus* (Linnaeus, 1767) has been subject to much debate (Bergsten et al., 2012; Drotz et al., 2001, 2010, 2012). Whatever their taxonomy, these beetles provide an excellent model system for exploring lineage diversification in mountain systems and the processes driving phenotypic and genetic divergence along altitudinal gradients, since *A. nevadensis* is restricted to high altitude waters and is completely surrounded by populations of *A. bipustulatus* at lower elevations in the region. *A. nevadensis* differs externally from *A. bipustulatus* on its smaller size, slenderer and more elongate body shape, secondary elytral reticulation pattern and the shape of male protarsal claws (Millán et al., 2014), although these characters vary somewhat in *A. bipustulatus* and the genitalia of the two taxa are almost identical. Angus et al. (2013) examined the karyotypes of several Dytiscidae species, and found no differences between *A. nevadensis* and *A. bipustulatus*. Intraspecific morphological variability across altitudinal gradients is common within the *A. bipustulatus* complex, with numerous forms of uncertain taxonomic status across its distributional range (Drotz et al., 2012). Most of these are presumably alpine, cold-adapted morphotypes, such as the *solieri* Aubé, 1837 or *kiesenwetterii* Seidlitz, 1887 forms, found in different mountain ranges of Europe (Balfour-Browne, 1950; Drotz et al., 2001, 2010; Sharp, 1882). In light of this variation, it has been suggested that *A. nevadensis* might also represent a morphotype of *A. bipustulatus* (Ribera et al., 1998); differences between the taxa reflecting intraspecific altitudinal variation rather than altitudinal speciation. *Agabus nevadensis* nests deeply within *A. bipustulatus* in gene fragment-based phylogenies (Bergsten et al., 2012; Drotz et al., 2010), but allozyme studies of the complex support the hypothesis of recent reproductive isolation between the two taxa (Drotz et al., 2010), making it difficult to distinguish between these possibilities at present.

Together with genomics and morphometrics, physiological characterisation of populations could be also useful in shedding light on unresolved species complexes, but has seldom been incorporated into integrative taxonomic studies (e.g. Chen & Hare, 2008; Degerlund et al., 2012; Muangmai et al., 2015). Whilst *A. nevadensis* is restricted to the high-mountain lakes of the Sierra Nevada (>2500 m), *A. bipustulatus* occupies a wider latitudinal and altitudinal range (from sea level to over 3500 m a.s.l., Table 1) across the Western Palearctic and occurs in all the main Iberian mountain systems and a wide diversity of freshwater habitats, including alpine lakes. Therefore, some degree of divergence in the environmental niche might be expected amongst these taxa (e.g. differing thermal tolerance, a critical aspect of a species fundamental niche; Arribas et al., 2012; Calosi et al., 2010).

The aim of this study was to use *A. nevadensis* and *A. bipustulatus* as a study system to analyse the role of Pleistocene climatic changes, local adaptation and phenotypic plasticity along elevation gradients on patterns of genomic and phenotypic variation in alpine taxa. To this end, we first used single nucleotide polymorphism (SNP) data from populations covering the entire altitudinal distribution range of *A. nevadensis* and multiple Iberian and trans-Palearctic populations of *A. bipustulatus* to (i) investigate spatial patterns of genetic structure and delineate lineages within the complex, (ii) infer their timing of diversification and past demographic history, and (iii) detect signatures of ongoing or historical hybridisation and genetic introgression among identified lineages. Second, we used geometric morphometrics and physiological experiments (thermal tolerance) to (iv) assess whether patterns of phenotypic variation are congruent with genomic-based inferences and the extent to which such variation is associated with phenotypic plasticity and/or local adaptation along altitudinal gradients.

2 | MATERIALS AND METHODS

2.1 | Study area and sampling

Our study area covers the Sierra Nevada mountain range in southeastern Iberia, to which the endemic *A. nevadensis* is restricted, and several populations of the widespread Western Palearctic *A. bipustulatus* (Table 1; Figure S1). We sampled 26 populations covering the full altitudinal range of each taxon in the Iberian Peninsula, from waterbodies located at sea level to alpine lakes in the major mountain ranges. Additionally, five populations of *A. bipustulatus* from other European regions and the Middle East were included (Table 1; Figure S1) and *Agabus bigutattus* (Olivier, 1795) was used as an outgroup in phylogenomic analyses. We used an aquatic hand net to collect eight to 12 specimens per locality. Specimens were stored in 96% ethanol and preserved at −20°C for genomic analyses. In a subset of localities where beetles were more abundant, additional specimens were collected for either morphometric and/or physiological analyses. The specific populations and sample sizes used for each analysis are presented in Table 1.

2.2 | Genomic library preparation and processing

We extracted and purified DNA from each specimen using NucleoSpin Tissue kits (Macherey-Nagel, Düren, Germany). We processed DNA of *A. nevadensis*, *A. bipustulatus* and *A. bigutattus* into different genomic libraries using the double-digestion restriction-fragment-based procedure (ddRAD-seq) described in Peterson et al. (2012). In brief, we digested DNA with the restriction enzymes MseI and EcoRI (New England Biolabs, Ipswich, MA, USA) and ligated Illumina adaptors including unique 7-bp barcodes to the digested fragments of each individual. We pooled ligation products, size-selected them between 350 and 450 bp with a Pippin Prep machine (Sage Science, Beverly, MA, USA) and amplified the fragments by PCR with 12 cycles using the iProofTM High-Fidelity DNA Polymerase (BIO-RAD, Veenendaal, The Netherlands). Single-read 201-bp sequencing was performed on an Illumina NovaSeq6000 platform. We used the different programs distributed as part of the STACKS v. 1.35 pipeline (Catchen et al., 2013) to filter and assemble our sequences into de novo loci, call genotypes, calculate genetic diversity statistics, and export input files for all downstream analyses. Unless otherwise indicated, we exported only the first SNP per RAD locus, and retained loci with a minimum stack depth ≥5 ($m=5$), a minimum minor allele frequency (MAF) ≥ 0.01 ($min\_maf=0.01$) and that were represented in at least 80% of the populations ($p=25$) and 50% of the individuals within each population ($r=0.5$). For more details on genomic data filtering and assembling, see Appendix S1.

2.3 | Analyses of genetic structure and admixture

We first performed a comprehensive suite of analyses to infer patterns of genetic structure, differentiation, admixture and hybridisation amongst studied lineages and populations. These included (i) genetic clustering analyses in STRUCTURE v. 2.3.3 (Pritchard et al., 2000), (ii) principal component analyses (PCA) of genetic variation (Jombart, 2008), (iii) estimates of genetic differentiation (F_{ST}) between populations, (iv) reconstructions of phylogenomic relationships amongstlineages/populations in SVDQUARTETS (Chifman & Kubatko, 2014) and (v) identification of hybrid categories using NEWHYBRIDS v.1.1 (Anderson & Thompson, 2002). Next, we analysed whether the probability of assignment of populations to the two genetic lineages coexisting within the Sierra Nevada mountain range (see section 3.2) is best explained by their geographical location and/or environmental factors.

2.3.1 | Genetic clustering analyses

We ran STRUCTURE analyses assuming correlated allele frequencies and admixture and without using prior population information. We conducted 15 independent runs for each value of K (from $K=1$ to $K=8$) to estimate the most likely number of genetic clusters with 200,000 MCMC cycles, following a burn-in step of 100,000

TABLE 1 Localities sampled and the number of individuals (*N*) used for genomic, geometric morphometric and physiological analyses.

	Locality							*N*		
Taxon	No	Code	Name	Country	Lat	Lon	Altitude (ma.s.l.)	Genomics	Geometric morphometry	Physiology
Agabus bipustulatus	1	IRAN	Stream near Ghachsar, Alborz Mts.	Iran	36.181	51.319	3500	8	5♀, 3♂	
A. bipustulatus	2	SARD	Río Pisciaroni, Sardinia	Italy	40.858	9.157	1030	8		
A. bipustulatus	3	ALPS	Pools nr. Chandolin, Alps	Switzerland	46.254	7.634	2400	10		
A. bipustulatus	4	PENN	Pools at High Cup Nick, Cumbria, Pennines	United Kingdom	54.643	−2.415	680	10		
A. bipustulatus	5	SOME	Ditch at Chilton Polden, Somerset	United Kingdom	51.177	−2.881	2	4	15♀, 15♂	
A. bipustulatus	6	AZUL	Ibón Azul Superior, Pyrenees	Spain	42.789	−0.246	2407	8	15♀,15♂	76
A. bipustulatus	7	ARME	Ibón de Armeña, Pyrenees	Spain	42.516	0.353	1850	10		
A. bipustulatus	8	LLOR	Lagos de Lloroza, Picos de Europa	Spain	43.164	−4.812	1870	8		
A. bipustulatus	9	MOLI	Pleta de Molières, Pyrenees	Spain	42.627	0.718	2000	10		
A. bipustulatus	10	MONE	Lago Moñetas, Picos de Europa	Spain	43.192	−4.789	1710	8		
A. bipustulatus	11	NEIL	Pool nr. Laguna Larga, Sierra de Neila	Spain	42.045	−3.061	1895	6		
A. bipustulatus	12	URBI	Zona encharcada en Laguna Helada, Picos de Urbión	Spain	41.995	−2.861	2000	8	13♀, 10♂	
A. bipustulatus	13	GRAN	Laguna Grande de Gredos, Sierra de Gredos	Spain	40.254	−5.275	1943	8	23♀, 15♂	70
A. bipustulatus	14	POZA	Prado de las Pozas, Sierra de Gredos	Spain	40.270	−5.246	1923	8		
A. bipustulatus	15	PENA	Pool nr. Laguna Grande de Peñalara, Sierra de Guadarrama	Spain	40.837	−3.951	1940	8		
A. bipustulatus	16	CLAV	Pools nr. Laguna de los Claveles, Sierra de Guadarrama	Spain	40.850	−3.948	2116	8	15♀,15♂	66
A. bipustulatus	17	PAJA	Laguna de los Pájaros, Sierra de Guadarrama	Spain	40.861	−3.948	2170	8		
A. bipustulatus	18	MURT	Río Múrtigas, La Nava, Huelva	Spain	37.957	−6.745	419	8	15♀, 15♂	22
A. bipustulatus	19	FSAL	Fuente Salobre, Albaida del Aljarafe, Sevilla	Spain	37.426	−6.165	163	8	3♀, 4♂	
A. bipustulatus	20	ESPU	Fuente Blanca, Sierra Espuña	Spain	37.886	−1.565	1142	9	24♀, 17♂	60
A. nevadensis	21	SJUA	Lagunillo de San Juan, Sierra Nevada	Spain	37.088	−3.372	2520	8		
A. nevadensis	22	LAVR	Laguna de los Lavaderos de la Reina, Sierra Nevada	Spain	37.124	−3.273	2635	10		
A. nevadensis	23	JUNT	Laguna de Juntillas, Sierra Nevada	Spain	37.110	−3.264	2930	8		
A. nevadensis	24	HOND	Laguna Hondera, Sierra Nevada	Spain	37.048	−3.294	2897	9		

TABLE 1 (Continued)

Taxon	Locality							N		
	No	Code	Name	Country	Lat	Lon	Altitude (ma.s.l.)	Genomics	Geometric morphometry	Physiology
A. nevadensis	25	MOSC	Laguna de la Mosca, Sierra Nevada	Spain	37.060	−3.315	2895	8		
A. nevadensis	26	CALD	Laguna de La Caldera, Sierra Nevada	Spain	37.055	−3.329	3030	9	18♀, 10♂	67
A. nevadensis	27	AVER	Laguna de Aguas Verdes, Sierra Nevada	Spain	37.049	−3.368	3055	8	14♀, 15♂	66
A. nevadensis	28	VIRG	Lagunillos de la Virgen, Sierra Nevada	Spain	37.053	−3.379	2945	8	12♀, 4♂	
A. nevadensis	29	MEDE	Lagunillo Medio de la Ermita, Sierra Nevada	Spain	37.050	−3.385	2870	8		
A. nevadensis	30	LLAN	Laguna de Lanjarón, Sierra Nevada	Spain	37.038	−3.400	2975	8		
A. nevadensis	31	CUAD	Laguna Cuadrada, Sierra Nevada	Spain	37.027	−3.419	2910	8	14♀, 13♂	

Note: A map of the study area is shown in Figure S1.

iterations. We retained the 10 runs having the highest likelihood for each value of *K* and determined the number of genetic clusters that best describes our data according to log probabilities of the data (LnPr(X|*K*); Pritchard et al., 2000) and the Δ*K* method (Evanno et al., 2005), as implemented in STRUCTURE HARVESTER v. 0.7 (Earl & vonHoldt, 2012). We used CLUMPP v. 1.1.2 and the Greedy algorithm to align multiple runs of STRUCTURE for the same *K* value (Jakobsson & Rosenberg, 2007) and DISTRUCT v. 1.1 (Rosenberg, 2004) to visualise the individuals' probabilities of population membership in bar plots.

2.3.2 | Principal component analyses of genetic variation

We ran a PCA of genetic variation as implemented in the R v. 4.2.3 (R Core Team, 2021) package *adegenet* v. 2.1.10 (Jombart, 2008). Before running the PCA, we replaced any missing data with the mean allele frequency of the corresponding locus estimated across all samples (Jombart, 2008).

2.3.3 | Genetic differentiation between populations

We calculated genetic differentiation between each pair of populations using the Weir and Cockerham weighted fixation index (F_{ST}; Weir & Cockerham, 1984) as implemented in ARLEQUIN v. 3.5 (Excoffier & Lischer, 2010). These analyses were performed for populations with a sample size of $n \geq 5$ after excluding those individuals identified by STRUCTURE as being hybrid/admixed (i.e. $q < 0.99$ for $K = 3$; see section 3.2). We determined statistical significance with Fisher's exact tests after 10,000 permutations, applying a false discovery rate adjustment (5%, $q < 0.05$) to control for multiple tests.

2.3.4 | Phylogenomic analyses

We ran SVDQUARTETS, as implemented in PAUP* v. 4.0a169 (Swofford, 2002), to estimate the relationships amongst populations and lineages identified by STRUCTURE (i.e. a population/species tree). To reduce the confounding effects of contemporary hybridisation on phylogenetic reconstructions, we excluded from the dataset hybrid/admixed individuals identified by STRUCTURE (i.e. $q < 0.99$ for $K = 3$; see section 3.2; e.g. Maier et al., 2019). We used *A. bigutattus* as an outgroup, evaluated 100,000 random quartets from the data set and quantified uncertainty in relationships using 100 bootstrapping replicates.

2.3.5 | Identification of hybrid categories

We performed a Bayesian assignment test of samples into discrete hybrid/parental categories using NEWHYBRIDS, which computes the

posterior probability (PP) distribution that each sample falls into one of six genotypic classes: parental classes (P1 and P2), first (F1) and second-generation (F2) hybrids, and backcrosses to both parental classes (BC1 and BC2). NEWHYBRIDS analyses were performed for two datasets, one including the trans-Palearctic and Iberian lineages of *A. bipustulatus* and another including the Iberian lineage of *A. bipustulatus* and *A. nevadensis* (see section 3.2). To overcome computational limitations of NEWHYBRIDS, we used the *gl.nhybrids* function in the R package *dartR* v. 2.9.7 (Gruber et al., 2018) to select the subset of 200 loci with the highest discriminatory power between parental classes. We considered as reference parental genotypes those individuals with a high probability of assignment ($q > 0.99$) to their respective genetic clusters, as inferred by STRUCTURE analyses for $K = 3$ (see section 3.2). We ran NEWHYBRIDS with default parameters and 50,000 MCMC steps after 10,000 burn-in steps on each of the two datasets.

2.3.6 | Drivers of genetic admixture within the Sierra Nevada

Some putative populations of *A. nevadensis* from the Sierra Nevada exhibited different degrees of admixed ancestry with the Iberian lineage of *A. bipustulatus* and, in some cases, even included purebred specimens of this lineage, that is, samples with a high probability of assignment (STRUCTURE q-value >0.99) to this genetic cluster (see section 3.2). For this reason, we used simple linear regressions to explore the relationship between the population-average probability of assignment to the Iberian lineage of *A. bipustulatus* and (i) climatic conditions, (ii) altitude and (iii) the 'accessibility' to each population from the lowlands, measured as the distance between the focal population and the 2500 m contour, a proxy of the distributional range limit of *A. nevadensis*. Climatic conditions were estimated using the 19 present-day bioclimatic variables downloaded from WorldClim v. 2.1 (Fick & Hijmans, 2017) at 30 arc-s resolution (ca. 1 km at the Equator) for the Sierra Nevada and its surroundings. We performed a PCA on bioclimatic variables and obtained, for each population, scores of the first principal component (PC), which explained 85% of the climatic variance and was mainly negatively correlated with mean annual temperature and the mean temperatures of the wettest, driest and coldest quarters and positively correlated with annual precipitation and precipitation in the driest and warmest quarters (see factor loadings in Table S1).

2.4 | Testing alternative models of lineage divergence

We used the coalescent-based approach implemented in FASTSIMCOAL2 (Excoffier et al., 2013) to test alternative models of divergence amongst *A. nevadensis* and the two lineages of *A. bipustulatus*. Specifically, we tested a model of divergence in strict isolation (SI) and models of isolation-with-migration considering either symmetric (IM_S) or asymmetric (IM_A) gene flow amongst lineages (Figure S2). For FASTSIMCOAL2 analyses we considered the three lineages inferred by STRUCTURE for $K = 3$ and the topology yielded by phylogenomic analyses in SVDQUARTETS (see section 3.2). These analyses aimed at investigating historical process of population divergence and genetic introgression amongst the three main lineages. For this reason, and in order to remove the confounding effects of contemporary hybridisation and recent admixture, we excluded all hybrid/admixed individuals from the dataset (i.e. STRUCTURE $q < 0.99$ for $K = 3$, as for phylogenomic reconstructions; see Results section; e.g. Bertola et al., 2024; Momigliano et al., 2021; Noguerales et al., 2024). Note also that including hybrid individuals (e.g. F1 and F2) in these analyses would require arbitrary decisions about how to assign them to each of the three discrete parental populations. Divergence times were estimated assuming two generations per year, although voltinism may decrease under unfavourable climatic conditions (Čiamporová-Zaovičová & Čiampor, 2011; Galewski & Tranda, 1978; Nilsson & Holmen, 1995). For details on FASTSIMCOAL2 analyses and model selection, see Appendix S2.

2.5 | Genetic diversity and past demographic history

First, we calculated different estimates of genetic diversity for each studied population (Table 1) using the program *populations* from STACKS (Catchen et al., 2013) and used one-way analyses of variance (ANOVAs) to test for significant differences in genetic diversity between the three lineages inferred by STRUCTURE analyses (see section 3.2). Second, we reconstructed the past demographic history from each lineage using the program STAIRWAY PLOT v. 2.1, which implements a flexible multi-epoch demographic model based on the site-frequency-spectrum (SFS) that does not require whole-genome sequence data or reference genome information (Liu & Fu, 2020). We computed the SFS for each lineage as described for FASTSIMCOAL2 analyses (Appendix S2) and ran STAIRWAY PLOT considering two generations per year, assuming a mutation rate of 2.8×10^{-9} per site per generation (Keightley et al., 2014), and performing 200 bootstrap replicates to estimate 95% confidence intervals.

2.6 | Geometric morphometric analyses

We used landmark-based geometric morphometric analyses to examine shape and size variation amongst (i) the two currently recognised taxa, (ii) the lineages inferred by genetic clustering analyses for $K = 3$ (section 3.2) and (iii) all sampled populations (Table 1). We excluded populations with hybrid/admixed individuals identified by STRUCTURE (i.e. $q < 0.99$ for $K = 3$) from these analyses. Unfortunately, the number of genotyped specimens per population ($n = 8$–10) was insufficient to perform robust morphometric analyses comparing purebred specimens with individuals

exhibiting different degrees of admixed ancestry (i.e. different early generation hybrid classes). We took digital images of the right elytron and captured 11 landmarks (2D configuration; Figure S3). We examined elytral shape as a proxy for body shape, which is one of the characters often use to distinguish between *Agabus* species (Millán et al., 2014). The coordinates of the landmarks were mapped onto images using TPSDIG v. 2.32 (Rohlf, 2015). We performed generalised Procrustes analyses to remove the effects of location, size, and rotation of the relative positions of landmarks amongst specimens. Centroid size was calculated as the square root of the sum of the square distances from the landmarks to the centroid that they defined (Zelditch et al., 2004) and was used as a proxy for specimen size. We tested for size differences amongst the currently recognised taxa, inferred lineages and populations, using ANOVAs with centroid size as the dependent variable, followed by post hoc pairwise comparisons.

We checked that our results on shape variation were not affected by the low sample sizes of some populations (Table 1) by using data from those populations with sample sizes >25 and estimating Procrustes distances between populations using (i) the full sample size and (ii) four randomly chosen specimens of each sex ($n = 100$ runs). Results showed no significant differences between observed and subsampled distances ($p > .05$). We used Procrustes ANOVA (Collyer et al., 2015; Goodall, 1991) to assess shape differences between the current taxa, the inferred lineages and the sampled populations. We used the residual randomisation permutation procedure (RRP) to estimate effect sizes and the significance of the terms (Anderson & Ter Braak, 2003). We then performed post hoc pairwise comparisons of Procrustes distance between lineages and populations. Additionally, we performed canonical variate analyses (CVA), which provides axes that maximise discrimination among groups (Zelditch et al., 2004), to visualise shape variation amongst inferred lineages and populations.

Finally, to assess the degree to which morphological variation is driven by local adaptation to altitudinal and climatic gradients, we explored the relationship between elytrum shape (scores of the first CV axis) and both altitude and climatic conditions across Iberian populations of the complex. Climatic conditions were estimated with a PCA using bioclimatic variables, as described in section 2.3.6, but for all Iberian populations. The scores from the first and second PCs, which together accounted for 77% of the climatic variance, were obtained for each population. PC1 was mainly negatively correlated with the maximum temperature of the warmest month and positively with annual precipitation and PC2 was negatively correlated with temperature seasonality and positively with minimum temperature of the coldest month (see factor loadings in Table S1).

For size and shape analyses, models were performed first including sex and its interaction with taxa, lineage or population as predictors. Then, as significant effects of sex were found (see section 3.5), each sex was analysed separately.

Morphometric analyses were performed in the R package *geomorph* v. 4.0.5 (Adams & Otarola-Castillo, 2013) and the software MORPHOJ v. 1.07a (Klingenberg, 2011).

2.7 | Thermal limits experiments

We compared the thermal tolerance (upper and lower thermal limits and their plasticity estimated through an experimental approach) between *A. nevadensis* and the Iberian lineage of *A. bipustulatus*. We used thermal tolerance data of several populations of *A. bipustulatus* from a previous study (Pallarés et al., 2024) and replicated the experimental procedure to obtain thermal limits of two populations of *A. nevadensis*. The populations used for these experiments (Table 1) only included purebred individuals of each corresponding lineage. Specimens of *A. nevadensis* were collected alive in summer 2022 and transported within 24 h to the laboratory in 500 mL containers with moistened filter paper, placed in a portable refrigerator at 10°C. Upon arrival, they were allowed to habituate to laboratory conditions for 3 days prior to experiments at 10°C and a 12:12 L:D photoperiod in a climatic chamber (SANYO MLR-351). Then, groups of individuals were acclimated at 10, 15 or 20°C for 7 days in climatic chambers. Maintenance conditions in the laboratory are described in Pallarés et al. (2024). After acclimation, sets of individuals were randomly divided in sub-groups of 10–15 beetles to estimate upper and lower thermal limits.

Heat tolerance was assessed by estimating the heat coma temperature (HCT) as the upper thermal limit. HCT, defined as the temperature at which individuals experience paralysis prior to death, preceded by spasmodic movements of legs and antennae (Chown & Terblanche, 2006), was estimated in air (i.e. on dry specimens), employing a dynamic method in which temperature is increased and the time to reach a specific physiological response is recorded (Lutterschmidt & Hutchison, 1997). We used a heating rate of 1°C/min. Body surface temperature at the moment of paralysis was measured with infrared thermography.

Cold tolerance was estimated using the supercooling point (SCP) as a lower thermal limit. SCP is the temperature at which the body fluids of the organism begin to freeze when specimens are exposed to cooling. SCP was estimated as the lower temperature reached before the release of the latent heat of crystallisation, employing also a dynamic method with a cooling rate of −1°C/min, and also using infrared thermography. Full details of each experiment are shown in Appendix S3 and Pallarés et al. (2024). All specimens were sexed after experiments and stored in 96% ethanol for use in morphometric analyses.

Differences in HCT and SCP amongst taxa and populations, and the effect of prior acclimation temperature, were determined using generalised linear models (GLMs) with a normal error structure and identity link function. Sex was also included as a fixed factor.

3 | RESULTS

3.1 | Genomic dataset

The average number of reads retained per individual after the different quality filtering steps was 2,724,121 (range = 154,963–7,169,390 reads). On average, this represented 81% (range = 49–90%) of the

total number of reads recovered for each individual. After filtering loci (see Appendix S1), the final dataset including all genotyped populations contained 1940 unlinked SNPs, with a mean coverage depth of 32× (mode = 34×; range = 6–58×) and an average proportion of missing data of 28% (mode = 19%; range = 14–70%).

3.2 | Analyses of genetic structure and admixture

STRUCTURE analyses showed that ΔK peaked at $K=2$ ($\Delta K=4680$) and $K=3$ ($\Delta K=1257$), followed by a sharp decline ($\Delta K<180$) at higher K-values (Figure S4). However, LnPr(X|K) increased from $K=2$ to $K=7$, reaching a plateau at $K=8$ (Figure S4). For $K=2$, one genetic cluster grouped the putative populations from *A. nevadensis* with the great majority of Iberian populations of *A. bipustulatus*, whereas the second genetic cluster included the populations of *A. bipustulatus* sampled across the rest of the Palearctic (hereafter, BIP-PAL, for simplicity; Figure 1a). All individuals from two populations from the Pyrenees (ARME and AZUL) were fully assigned ($q>0.99$) to the genetic cluster BIP-PAL mostly represented in extra-Iberian populations. Remarkably, individuals with a high probability of assignment ($q>0.90$) to each of the two genetic clusters were syntopic in two populations from the Cantabrian Mountains (LLOR and MONE) in North Iberia (Figure 1a). Several populations (PENN, SOME, SARD, LLOR and MOLI) presented individuals with different degrees of admixed ancestry between the two lineages of *A. bipustulatus*, suggesting ongoing or historical hybridisation and introgression (Figure 1a). For $K=3$, most putative populations of *A. nevadensis* (hereafter, NEV) split from Iberian populations of *A. bipustulatus* (hereafter, BIP-IBE). However, several individuals sampled in putative populations of *A. nevadensis* (SJUA, LAVR and HOND) were assigned with a high probability of membership ($q>0.99$) to the genetic cluster BIP-IBE mostly represented in Iberian populations of *A. bipustulatus*; in these populations, individuals assigned with a high probability of membership to both genetic clusters were syntopic (Figure 1b,e). Several populations from Sierra Nevada also contained individuals with different degrees of admixed ancestry between these two clusters, indicating ongoing hybridisation and introgression (Figure 1b,e). STRUCTURE analyses for higher K-values ($K=4$–7) revealed further genetic structure (Figure S5).

The PCA yielded results in line with those obtained for STRUCTURE, separating three genetic clusters corresponding with the lineages BIP-PAL, BIP-IBE and NEV (Figure 1f). PC1 separated the lineage BIP-PAL from the lineages BIP-IBE and NEV, PC2 separated BIP-IBE from NEV, and some samples with intermediate PC scores corresponding to admixed/hybrid individuals (Figure 1f).

Except for three comparisons involving one population of BIP-IBE (MOLI) and three populations of NEV (MOSC, AVER and VIRG), all pairwise F_{ST} values involving populations assigned to different lineages were significantly different from zero (F_{ST} range: 0.025–0.606; Table S2). All pairwise F_{ST} values between populations of BIP-PAL were significantly different from zero (F_{ST} range: 0.084–0.569; Table S2). Except for a few comparisons involving the nearby populations AVER, VIRG and LLAN, all pairwise F_{ST} values between populations of the lineage NEV were also significantly different from zero (F_{ST} range: 0.000–0.268; Table S2). In contrast, no pairwise F_{ST} values between populations of BIP-IBE were significantly different from zero (F_{ST} range: 0.000–0.016; Table S2).

Phylogenomic analyses in SVDQUARTETS supported the results from STRUCTURE and revealed that *A. nevadensis* is nested within *A. bipustulatus*, which is a paraphyletic taxon (Figure S6). The trans-Palearctic lineage of *A. bipustulatus* (BIP-PAL) is sister to a clade including the Iberian lineage of *A. bipustulatus* (BIP-IBE) and *A. nevadensis* (NEV), which are sister lineages (Figure S6). However, the phylogenetic relationships amongst lineages and populations were not well resolved in most cases (bootstrap support <95%) and one population of *A. bipustulatus* sympatric with *A. nevadensis* was included within the clade of *A. nevadensis* with a basal relationship with the rest of the populations.

NEWHYBRIDS analyses for the BIP-PAL and BIP-IBE dataset unambiguously assigned (PP > 0.95) one individual from the population MOLI to a backcross (BC) with BIP-IBE, 66 individuals to BIP-PAL, and 96 individuals to BIP-IBE (Figure 1c). NEWHYBRIDS analyses for the BIP-IBE and NEV dataset unambiguously assigned (PP > 0.95) four individuals to second generation hybrids (F2), 83 individuals to the BIP-IBE lineage, and 66 individuals to the NEV lineage. The remaining 18 samples could not be unambiguously assigned to a single genotypic class (PP < 0.95; Figure 1d). These results suggest that the admixture identified by STRUCTURE in several individuals, especially those collected outside the Sierra Nevada (e.g. SOME, PENN, and LLOR), is probably due to shared ancestral alleles (i.e. retained ancestry) rather than a consequence of hybridisation.

In the Sierra Nevada populations, the mean probability of assignment to the genetic cluster corresponding to the BIP-IBE lineage showed significant negative correlations with (i) the first PC summarising climatic conditions (slope ± S.D. = −0.055 ± 0.016, $p=.006$, $R^2=.533$, $n=11$), which mainly summarises annual and seasonal temperature and precipitation variables (Table S1), (ii) the distance to the 2500 m isohyet (slope ± S.D. = −0.0003 ± 0.0001, $p=.017$, $R^2=.429$, $n=11$) and (iii) altitude (slope ± S.D. = −0.002 ± 0.0002, $p<.001$, $R^2=.821$, $n=11$; Figure S7).

3.3 | Testing alternative models of lineage divergence

The model best explaining the formation of the three lineages of *A. nevadensis* and *A. bipustulatus* is a scenario of isolation-with-migration and asymmetric gene flow (IM_A; Table 2; Figure 2); other tested models receiving much lower statistical support (ΔAIC >99; Table 2). Considering two generations per year, the split of the BIP-PAL from the two other lineages was estimated to have taken place during the last glacial period (ca. 57 ka), whereas the Iberian lineages BIP-IBE and NEV diverged at the end of the last glacial period (ca. 14 ka; Table 3; Figure 2). Effective migration rates per generation between demes were asymmetric and significantly different (i.e. 95% confidence intervals do not overlap; Table 3). Remarkably, gene flow from BIP-IBE to NEV was five-fold higher than in the opposite direction (Table 3; Figure 2).

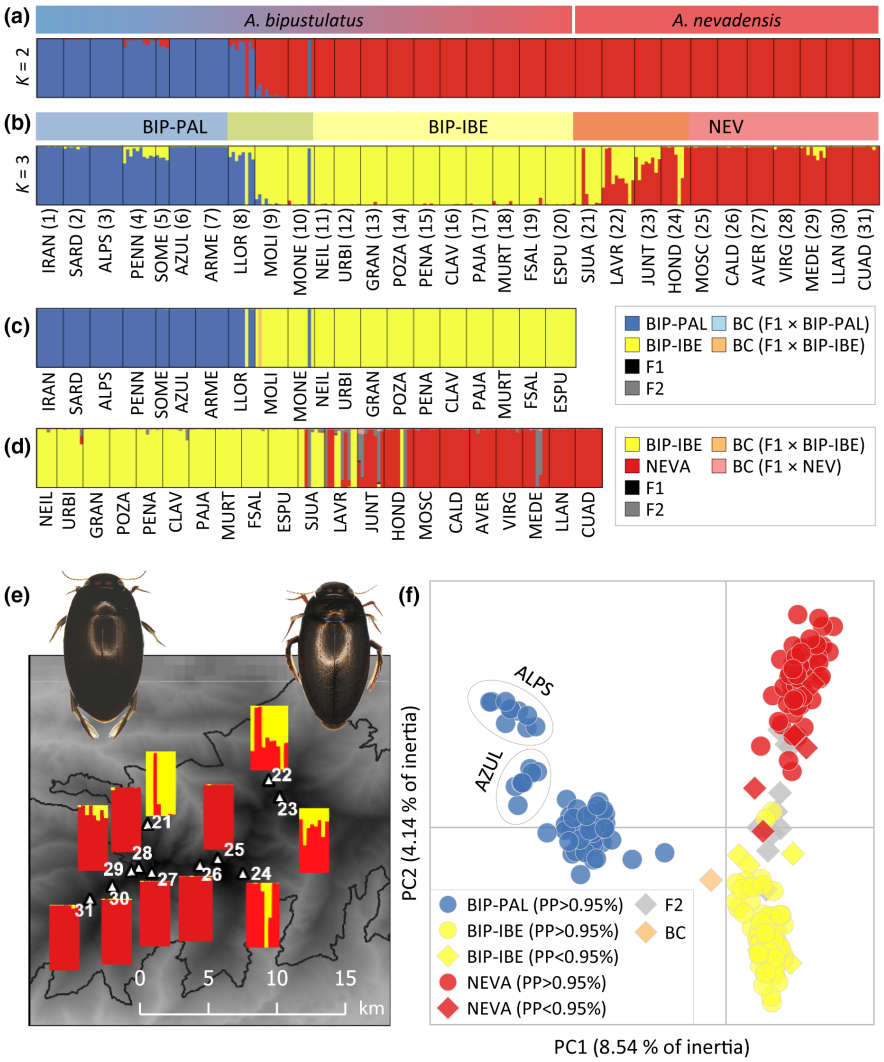

FIGURE 1 Results of genetic structure and admixture analyses. (a, b) Genetic assignments based on STRUCTURE for (a) $K=2$ and (b) $K=3$; species names, as traditionally assigned; each individual is represented by a vertical bar, which is partitioned into K coloured segments showing the individual's probability of belonging to the cluster with that colour. (c, d) Genetic assignments based on NEWHYBRIDS for comparisons involving (c) the trans-Palearctic (BIP-PAL) and Iberian (BIP-IBE) lineages of *A. bipustulatus* and (d) BIP-IBE and *A. nevadensis* (NEV). Each individual is represented by a vertical bar, which is partitioned into K coloured segments showing the individual's probability of belonging to each of the six genotypic classes inferred: P1, P2, F1, F2, BC1 and BC2 (for details, see section 2.3.5). (e) Genetic assignment of individuals from populations in the Sierra Nevada, as inferred from STRUCTURE for $K=3$. The black line represents the 2500 m contour. Insect images show *A. bipustulatus* (left) and *A. nevadensis* (right) (author: JA Carbonell). (f) principal component analysis (PCA) of genetic variation. Shapes and colours in the PCA correspond to the genotypic classes assigned in NEWHYBRIDS analyses. Dots indicate individuals unambiguously assigned (PP > 0.95) to one of the parental genotypes (P1 or P2). Yellow and red diamonds indicate individuals that were mostly, but not unambiguously (0.95 > PP > 0.70), assigned to BIP-IBE and NEV, respectively. Grey diamonds correspond to F2 individuals involving hybridisation between BIP-IBE and NEV (see (c)) and the light red diamond corresponds to a backcross resulted from hybridisation between BIP-IBE and BIP-PAL (see (d)). With the exception of populations ALPS and AZUL from BIP-PAL (ellipses), other populations within each lineage largely overlap in the PCA and are not outlined for the sake of clarity. Population codes as described in Table 1.

3.4 | Genetic diversity and past demographic history

Genetic diversity statistics are presented in Table S3. Genetic diversity differed amongst populations assigned to the three lineages (one-way ANOVAs; H_O: $F_{2,20}=6.05$, $p=.009$; H_E: $F_{2,20}=7.21$, $p=.004$; π: $F_{2,20}=7.95$, $p=.003$; F_{IS}: $F_{2,20}=8.33$, $p=.002$). Post hoc Tukey's tests revealed that these differences were due to the higher levels of genetic diversity in the Iberian lineage of *A. bipustulatus* than in the trans-Palearctic lineage of *A. bipustulatus* (H_O: $p=.007$; H_E: $p=.004$; π: $p=.003$; F_{IS}: $p=.006$) and *A. nevadensis* (F_{IS}: $p=.011$; for all other statistics, p-values >.05). STAIRWAY PLOT analyses showed that the three lineages have experienced demographic expansions just before (trans-Palearctic lineage of *A. bipustulatus*) or just after (Iberian lineage of *A. bipustulatus* and *A. nevadensis*) the last glacial maximum (LGM), followed by demographic stability since the onset

TABLE 2 Alternative models of divergence for *Agabus nevadensis* and the Iberian and trans-Palearctic lineages of *A. bipustulatus* tested using FASTSIMCOAL2, with the best-supported scenario highlighted in bold.

Model	Scenario	Migration	lnL	*k*	AIC	ΔAIC	ω_i
Model 1 (SI)	Strict isolation	–	−3588.93	6	7189.87	209.55	0.00
Model 2 (IM_S)	Isolation-with-migration	Symmetric	−3531.66	8	7079.32	99.00	0.00
Model 3 (IM_A)	**Isolation-with-migration**	**Asymmetric**	**−3480.16**	**10**	**6980.32**	**0.00**	**1.00**

Note: Models include scenarios of divergence in strict isolation (SI) and isolation-with-migration (IM) considering either symmetric (IM_S) or asymmetric (IM_A) gene flow (illustrated in Figure S2).

Abbreviations: ΔAIC, difference in AIC value from that of the strongest model; AIC, Akaike's information criterion value; *k*, number of parameters in the model; lnL, maximum likelihood value of the model; ωi, AIC weight.

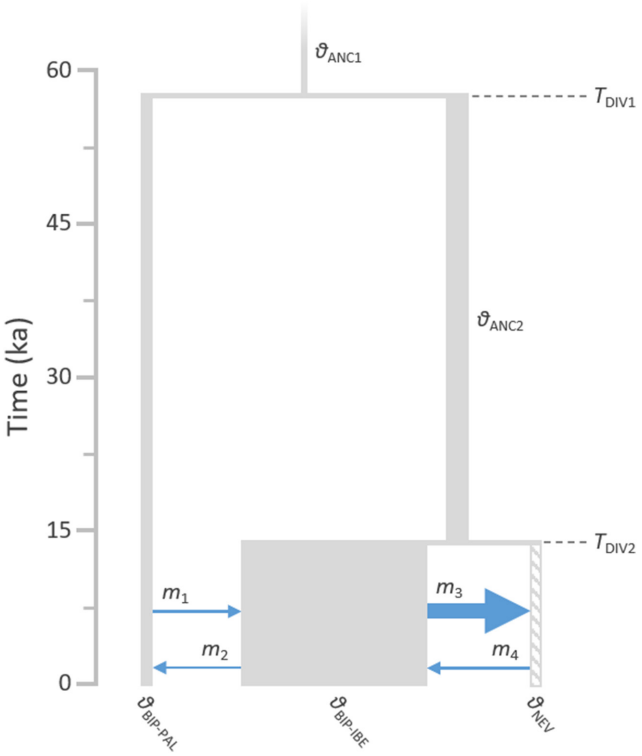

FIGURE 2 Schematic of the best supported model (i.e. isolation-with-migration and asymmetric gene flow, IM_A; see Table 2) of divergence for *Agabus nevadensis* (NEV) and the Iberian (BIP-IBE) and trans-Palearctic lineages (BIP-PAL) of *A. bipustulatus*. Parameters include mutation-scaled ancestral (θ_{ANC1} and θ_{ANC1}) and contemporary effective population sizes ($\theta_{BIP\text{-}PAL}$, $\theta_{BIP\text{-}IBE}$ and θ_{NEV}), effective migration rates per generation (m_1, m_2, m_3 and m_4), and timing of divergence (T_{DIV1} and T_{DIV2}). Point estimates yielded by FASTSIMCOAL2 were used to scale the different time events (*T*, left axis), effective population sizes (θ, proportional to branch width) and effective migration rates per generation (*m*, proportional to arrow thickness). Migration rates (*m*) are presented as 2 Nm and estimates of time are given in years, assuming two generations per year. Demographic parameter values and confidence intervals are detailed in Table 3. Contemporary effective population size of *A. nevadensis* (θ_{NEV}, hatched box) was calculated from levels of nucleotide diversity (π) and fixed in FASTSIMCOAL2 analyses to enable estimation of other parameters (see section 2.4 for further details).

of the Holocene (Figure 3). Only the Iberian lineage of *A. bipustulatus* may have experienced recent demographic declines (<1000 years ago), although the wide confidence intervals do not exclude the possibility of demographic stability here (Figure 3).

TABLE 3 Parameters inferred from coalescent simulations with FASTSIMCOAL2 under the most supported scenario of divergence (i.e. isolation-with-migration considering asymmetric gene flow, IM_A; see Table 2) for *Agabus nevadensis* (NEV) and the Iberian (BIP-IBE) and trans-Palearctic (BIP-PAL) lineages of *A. bipustulatus*.

Parameter	Point estimate	Lower bound	Upper bound
θ_{ANC1}	36,188	26,902	32,981
θ_{ANC2}	129,298	119,131	130,573
$\theta_{BIP\text{-}PAL}$	68,680	65,753	71,785
$\theta_{BIP\text{-}IBE}$	1,047,098	925,000	993,379
θ_{NEV}	53,571	–	–
T_{DIV1}	57,330	58,209	64,482
T_{DIV2}	14,202	14,172	15,456
$m_{1\ (BIP\text{-}PAL \rightarrow BIP\text{-}IBE)}$	1.54	1.47	1.54
$m_{2\ (BIP\text{-}PAL \leftarrow BIP\text{-}IBE)}$	1.00	0.86	0.97
$m_{3\ (BIP\text{-}IBE \rightarrow NEV)}$	6.68	5.95	6.84
$m_{4\ (BIP\text{-}IBE \leftarrow NEV)}$	1.24	1.11	1.21

Note: Table shows point estimates and lower and upper 95% confidence intervals for each parameter, which include mutation-scaled ancestral (θ_{ANC1} and θ_{ANC1}) and contemporary effective population sizes ($\theta_{BIP\text{-}PAL}$, $\theta_{BIP\text{-}IBE}$, and θ_{NEV}), effective migration rates per generation (m_1, m_2, m_3 and m_4, with direction of gene flow between demes indicated in parentheses), and timing of divergence (T_{DIV1} and T_{DIV2}). Parameters are illustrated in Figure 3. Migration rates (*m*) are presented as 2 Nm and estimates of time are given in years, assuming two generations per year. Note that the contemporary effective population size of *A. nevadensis* (θ_{NEV}) was calculated from levels of nucleotide diversity (π) and fixed in FASTSIMCOAL2 analyses to enable the estimation of other parameters (see section 2.4 for further details).

3.5 | Geometric morphometric analyses

Significant differences in centroid size were found between currently recognised taxa (specimens of *A. bipustulatus* being on average 11% bigger than specimens of *A. nevadensis*, ♀: $F_{1,181}=385.1$, $p<.001$; ♂: $F_{1,144}=124.1$, $p<.001$), the three lineages inferred from genetic clustering analyses (♀: $F_{2,180}=190.4$, $p<.001$; ♂: $F_{2,143}=126.4$, $p<.001$; NEV < BIP-PAL < BIP-IBE, all *p*s < .05 in post-hoc tests) and populations (♀: $F_{12,170}=41.7$, $p<.001$; ♂: $F_{12,133}=25.5$, $p<.001$). Full model results are shown in Table S4.

Procrustes ANOVA (Table S5) showed significant differences in elytral shape between currently recognised taxa (♀: $F_{1,181}=32.4$, $p=.001$; ♂: $F_{1,144}=28.6$, $p=.001$), inferred lineages (♀: $F_{2,180}=36.9$, $p=.001$; ♂:

$F_{2,143}$=31.4, p=.001) and populations (♀: $F_{12,170}$=10.2, p<.001; ♂: $F_{12,133}$=8.8, p=.001). All pairs of inferred lineages differed significantly in post-hoc tests, both in females (Table S6) and males (Table S7). In post-hoc tests comparing pairs of populations, in general, no differences were found between population pairs belonging to the same lineage, whilst most population pairs from different lineages showed significantly different elytral shapes, in both sexes (Tables S6 and S7).

The first two canonical axes of the CVA explained 74.4% and 73.1% of variation in elytral shape amongst the three lineages inferred by genetic clustering analyses in females and males respectively. CVA plots showed clearly differentiated morphotypes corresponding to the three lineages, with slight overlap, in both sexes (Figure 4). Elytra varied along the first axis from a wider shape in the BIP-IBE to a narrower, more elongated one in the NEV and BIP-PAL groups; whilst these latter two groups were separated along the second axis (Figure 4). CVA amongst populations showed a high overlap between populations within each inferred lineage, especially within the NEV and BIP-IBE groups (Figure S8). Elytral shape in the NEV and BIP-IBE lineages was significantly correlated with altitude in both sexes; however, this relationship was disproportionately influenced by populations of *A. nevadensis* and did not hold significant when these were removed from the analysis (see Table S8). No relationship was found between elytral shape and climatic conditions (Table S8).

3.6 | Thermal limits experiments

Heat coma temperature was 0.7°C higher, on average, in *A. nevadensis* than in the Iberian lineage of *A. bipustulatus*, this difference being statistically significant ($F_{1,202}$=35.923, p<.001). Females' HCT values were

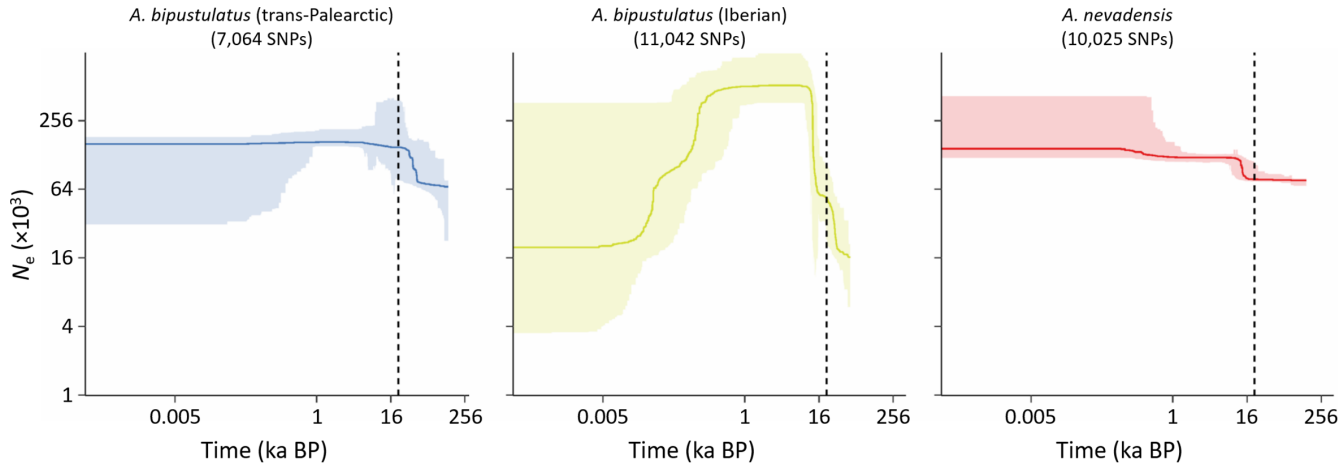

FIGURE 3 Demographic reconstructions inferred using STAIRWAY PLOT for *Agabus nevadensis* and the Iberian and trans-Palearctic lineages of *A. bipustulatus*. Plots show median (solid lines) and 2.5 and 97.5 percentiles (shaded areas) of effective population size (N_e) through time, estimated assuming a genomic mutation rate of 2.8×10^{-9} per site per generation and two generations per year (both axes in logarithmic scale). Vertical dashed lines indicate the Last Glacial Maximum (LGM; ca. 21 ka). The number of polymorphic SNPs used to calculate the site frequency spectrum (SFS) is indicated in parentheses.

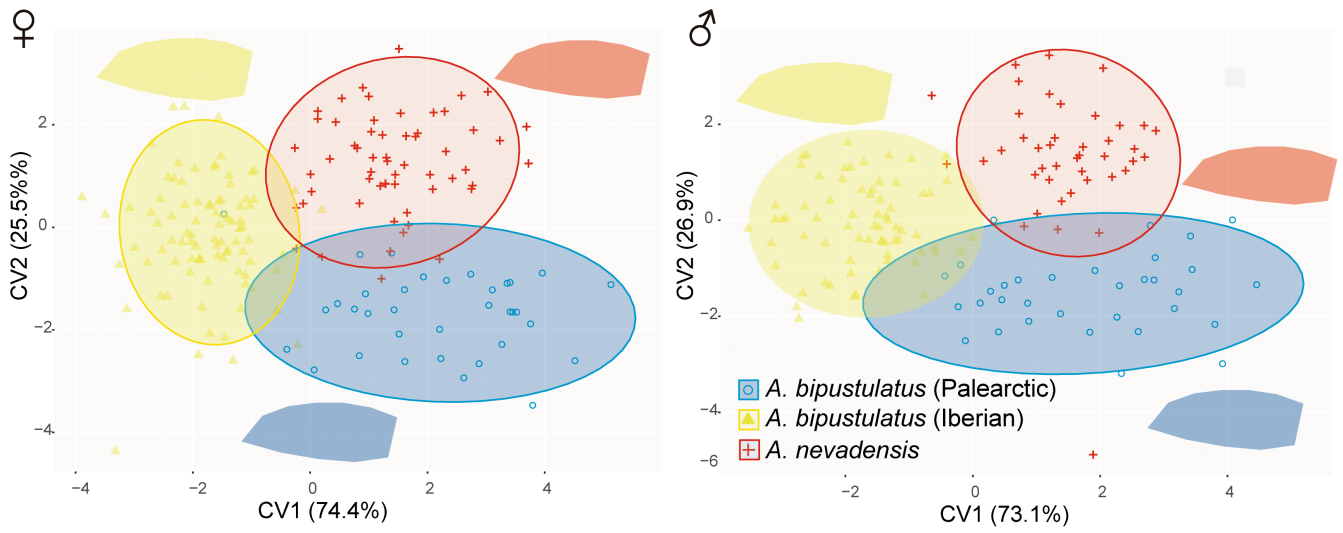

FIGURE 4 Elytral shape of females and males from the different lineages (as inferred from STRUCTURE for K=3), represented by the first two canonical variate analyses (CVA) axes. 95% confidence ellipses are shown. The wireframe plots represent the mean shape of the elytra in each lineage.

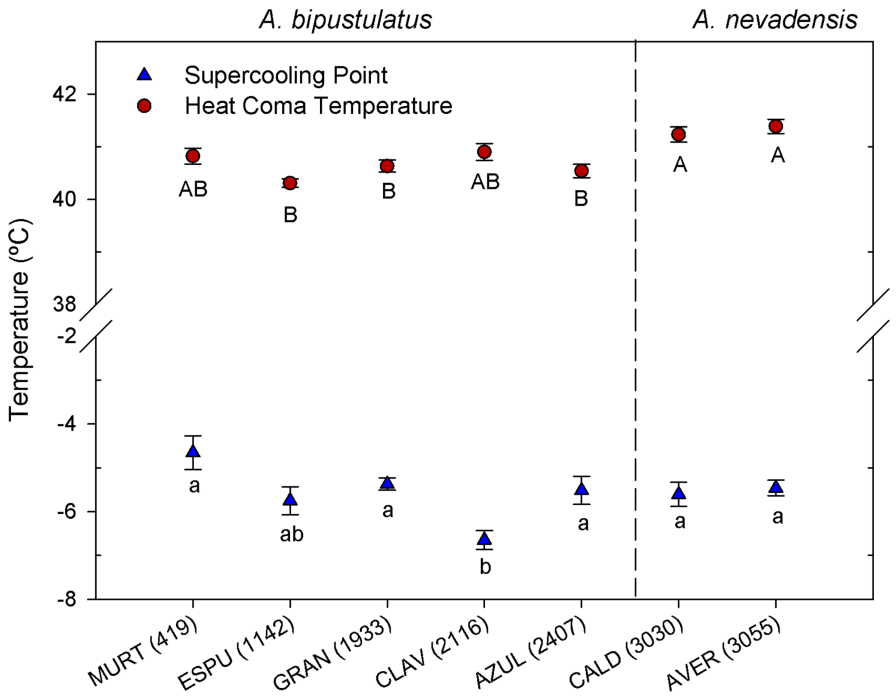

FIGURE 5 Upper (heat coma temperature) and lower (supercooling point) thermal limits of populations of the Iberian lineage of *Agabus bipustulatus* and *A. nevadensis* along an altitudinal gradient. Mean ± SD values are shown. The *x*-axis shows populations ordered from lower to higher altitude (shown as m a.s.l. in parentheses; codes as described in Table 1). Significant differences between populations (Bonferroni *p*-adjusted <.05) are indicated with capital and lower-case letters for upper and lower thermal limits respectively.

on average 0.4°C higher than those of males in both taxa ($F_{1,199}=9.287$; $p=.003$; Tables S9 and S10). GLM comparing populations, irrespective of taxon, showed significant differences amongst them ($F_{6,197}=8.323$, $p<.001$). The two high-altitude populations of *A. nevadensis* showed the highest HCTs and three populations of *A. bipustulatus* showed the lowest values, with the remaining two populations of the latter showing intermediate HCTs (Figure 5). No significant effect of acclimation temperature nor its interaction with species, population, sex or with all factors was found (see full GLMs results in Table S10).

Regarding cold tolerance, SCP values did not differ between taxa, sexes or acclimation treatments, but significant differences amongst populations were found ($F_{6,167}=4.454$, $p<.001$; Tables S9 and S10), mainly attributed to the significantly lowest SCP of one population of *A. bipustulatus* (CLAV) with respect to the rest (Figure 5).

4 | DISCUSSION

Our genomic analyses reveal the existence of three recently diverged lineages amongst populations of the studied diving beetles. Multiple lines of evidence suggest that *A. nevadensis* is an alpine 'ecotype' of *A. bipustulatus* resulting from an incipient speciation process. Genomic inferences are supported by differences between lineages in both morphological and thermal tolerance traits, which suggest that adaptation to alpine environments has contributed to phenotypic differentiation.

4.1 | Lineage diversification and admixture

According to genetic structure analyses, the sampled populations comprise three geographically coherent genetic clusters. In the Sierra Nevada, the highest altitude populations were assigned to a cluster corresponding to the narrowly endemic *A. nevadensis*. This taxon was syntopic with a sister lineage of *A. bipustulatus* in localities at lower elevations in this mountain range, where the two hybridised and even formed hybrid swarms. This result is consistent with previous records of specimens of uncertain taxonomic identity between *A. nevadensis* and *A. bipustulatus* from lower altitudes in the Sierra Nevada (P. Abellán & A. Millán, Personal observations). Sampled populations of *A. bipustulatus* split into two lineages, one exclusively distributed in the Iberian Peninsula (BIP-IBE) and another encompassing the remaining Palearctic populations as far East as Iran (BIP-PAL), with genetic admixture at contact zones located in the Pyrenees and Cantabrian Mountains. Remarkably, purebred individuals of the different lineages were syntopic in some localities (e.g. HOND and MONE), suggesting that reproductive isolation, even if still incomplete, may contribute to lineage persistence in areas of secondary contact (Dynesius & Jansson, 2014). However, we cannot entirely discard the possibility that such purebred specimens are first generation immigrants that dispersed from other localities. In agreement with genetic structure analyses, phylogenomic reconstructions show a major split between Iberian and Palearctic lineages, and a subsequent divergence between the Sierra Nevada and the remaining Iberian populations, recovered as reciprocally monophyletic clades albeit with low node support, likely due to recent divergence and introgression. *A. bipustulatus*, as currently defined, would therefore be a paraphyletic taxon, in line with mtDNA-based phylogenies in which *A. nevadensis* is nested within *A. bipustulatus* (Bergsten et al., 2012; Drotz et al., 2010).

The best supported model of lineage divergence was one assuming isolation-with-migration and asymmetric gene flow. Divergence times estimated under this model suggest that the

Iberian populations of *A. bipustulatus* split around 60,000 years ago, which is consistent with the Iberian Peninsula functioning as a refugial area for temperate taxa during Quaternary glaciations (Gómez & Lunt, 2007; Hewitt, 1999). The role of the Iberian Peninsula as an important glacial refugia is also supported by the higher levels of genetic diversity in the Iberian lineage of *A. bipustulatus* compared to the estimates obtained for populations of the trans-Palearctic lineage, which have likely sustained lower effective population sizes through time and experienced losses of genetic diversity during post-glacial northward expansions (i.e. the 'northern purity, southern richness' paradigm; Hewitt, 1999). In line with the 'refugia within refugia' concept (Abellán & Svenning, 2014; Gómez & Lunt, 2007), Iberian populations of *A. bipustulatus* likely underwent shifts towards higher elevations during unfavourable periods and became fragmented in isolated patches of suitable habitat at high elevations, like the Sierra Nevada. This appears a plausible scenario for the origin of the microendemic *A. nevadensis*, which according to demographic models, diverged from the Iberian lineage of *A. bipustulatus* around 14,000 years ago (at the end of the last glacial period). Successive cycles of range expansion–fragmentation have been proposed as an important mechanism driving diversification for cold-adapted species in Europe (Ortego & Knowles, 2022; Schmitt, 2007), and this appears to be also the case with some aquatic insects in the Iberian Peninsula (García-Vázquez et al., 2017; Ribera & Vogler, 2004). For example, various lineages within the water beetle genus *Hydraena* underwent diversification in the Peninsula during periods of range contraction of more widely distributed ancestors, leading to the emergence of multiple isolated narrow range endemics, including *Hydraena tatii* Sainz-Cantero & Alba-Tercedor, 1989, confined to Sierra Nevada and nearby mountains (Ribera et al., 2011). Similarly, the diversification of the caddisfly genus *Annitella* is linked to southern and extra-Mediterranean refugia across Europe during the Pleistocene, and includes two endemic species restricted to the Sierra Nevada, *Annitella iglesiasi* González & Malicky 1988 and *A. esparraguera* (Schmid 1952), which likely originated as a consequence of ancestral range fragmentation during interglacial periods (Múrria et al., 2020).

A number of studies have provided evidence indicating the pivotal role of the Sierra Nevada as a refuge for insect populations during the Quaternary glacial–interglacial cycles, safeguarding ancestral populations from introgressive dispersal events that were common in other parts of the continent (Arroyo et al., 2022). However, our analyses demonstrate the presence of hybridisation between *A. nevadensis* and *A. bipustulatus* in these mountains, suggesting that reproductive barriers between these beetles are incomplete and have been permeable during their evolutionary history. Collectively, our results are in agreement with the idea of the Sierra Nevada functioning as a 'sky island' (Love et al., 2023), an isolated mountain range separated from others by lowlands with unsuitable environmental conditions during interglacial periods, in which changing climatic conditions lead to alternating periods of population isolation and connectivity, as documented for many alpine taxa (e.g. Hedin et al., 2015; Tonzo & Ortego, 2021).

The effective migration rates estimated by demographic models were much higher from the Iberian lineage of *A. bipustulatus* to *A. nevadensis* than in the opposite direction. Such an asymmetric pattern of gene flow has been reported for other taxa (e.g. Alves et al., 2008; Lukicheva & Mardulyn, 2021; Ortego et al., 2021), and could perhaps be expected in a situation where populations of a narrow range endemic taxon (*A. nevadensis*, restricted to alpine habitats) are surrounded by a widely distributed relative (*A. bipustulatus*, distributed from lowlands to alpine habitats). Our results suggest that the complex topography of the Sierra Nevada may play a role in limiting introgression to those areas most accessible from the lowlands. The asymmetric gene flow may also result from differences in the relative regional abundance of the two forms, or differences in their dispersal propensity. Drotz et al. (2001) suggested that alpine populations of *A. bipustulatus* in Scandinavia fly less than their lowland counterparts, something that may also apply in the Sierra Nevada. Whilst *A. nevadensis* apparently has functional wings, which are not markedly distinct from those of *A. bipustulatus* (P. Abellán, Personal observations), further research is necessary to determine whether both taxa exhibit contrasting dispersal abilities. An important question here is how the current interaction between lineages could impact the long-term persistence of *A. nevadensis*. Secondary contact zones may maintain lineage integrity, lead to the formation of new hybrid taxa or homogenise lineages ('lineage fusion' or 'speciation reversal'; Maier et al., 2019). Several studies have provided support for these phenomena in different taxa (e.g. Behm et al., 2010; Garrick et al., 2014; Vonlanthen et al., 2012; Webb et al., 2011), including alpine lineages (e.g. Maier et al., 2019; Noguerales & Ortego, 2022). Indeed, in the case of young lineages, such as those studied here, lineage fusion seems to dominate, particularly when reproductive isolation is weak (Garrick et al., 2014; Kearns et al., 2018; Seehausen et al., 2008). This could be particularly relevant in a context of global change, as most cases of speciation reversal are linked to recent anthropogenic causes such as climate change and habitat loss (e.g. Kleindorfer et al., 2014; Taylor et al., 2006).

4.2 | Morphological and physiological differentiation

Geometric morphometric analyses and thermal tolerance experiments suggest that, alongside periods of geographical isolation between lineages during Quaternary glacial–interglacial cycles (see section 4.1), local altitudinal selection may have contributed to phenotypic differentiation.

Geometric morphometrics allowed us to detect subtle, but significant body shape differences between the studied taxa and identify three distinct morphotypes corresponding to the three lineages inferred through genomic analyses. The most evident

morphological difference, which was consistent in both sexes, was the wider elytra shape of the Iberian lineage of *A. bipustulatus* compared to the more elongate and narrowed elytra of *A. nevadensis* and the trans-Palearctic lineage of *A. bipustulatus* (Figure 4). The two latter lineages separated along the second CVA axis but showed more subtle shape differences, difficult to detect with the naked eye (Figure 4). Interestingly, elytral shape was significantly correlated with altitude across Iberian populations (i.e. including both the BIP-IBE and NEV lineages), but this correlation was not significant when populations of *A. nevadensis* were excluded from the analysis. This suggests that phenotypic differentiation of *A. nevadensis* could have resulted from a micro-evolutionary process of local altitudinal adaptation that has not been replicated in other alpine populations of its sister lineage of Iberian *A. bipustulatus*. This finding contrasts with patterns of phenotypic variation in other morphological traits within the *A. bipustulatus* complex (Drotz et al., 2001; Drotz et al., 2012) or the genus *Agabus* more generally (Nilsson & Persson, 1990), along elevation gradients. For example, elytral reticulation patterns in *A. nevadensis* are similar to those of northern European alpine forms of *A. bipustulatus* (Drotz et al., 2010), something that has been attributed to parallel altitudinal selection processes within the species complex. We cannot rule out a parallel altitudinal process of elytral shape differentiation between *A. nevadensis* and *A. bipustulatus* populations outside Iberia, since the trans-Palearctic lineage of *A. bipustulatus* appears to be morphologically more similar to *A. nevadensis* than to the Iberian *A. bipustulatus*, as indicated above. However, the limited representation of the trans-Palearctic lineage in our dataset prevents us from exploring this in any detail.

Understanding the full ecological and functional significance of body shape differences observed between lineages was outside the scope of our study. That said, body shape is well known to be related to habitat preferences in diving beetles (Ribera et al., 1997; Ribera & Nilsson, 1995), with elongate, more narrow-bodies species being stronger, faster swimmers living in relatively open water, and shorter, more compact taxa being more manoeuvrable and often found in dense vegetation (Miller & Bergsten, 2016). It is possible, therefore, that the relatively slender body shape found in *A. nevadensis* compared to Iberian *A. bipustulatus* represents an adaptation to live in relatively open water, lacking dense macrophytes, as is the case in alpine lakes.

As foreseen with body shape, thermal niche also differed between *A. nevadensis* and the Iberian lineage of *A. bipustulatus*. According to our experiments, *A. nevadensis* has a wider thermal tolerance range than *A. bipustulatus*, due to its higher upper thermal limit, even though the former occupies a much narrower elevational range and climatic niche than the latter. Although different patterns have been documented for some other insects, in which high altitude populations or species show lower or similar heat tolerance than those at lower elevations (e.g. some terrestrial beetles: Slatyer & Schoville, 2016; bees: Gonzalez et al., 2022), our findings are consistent with previous work on other aquatic insects. Some high-elevation species of dytiscids (Carbonell et al., 2024) and mayflies, stoneflies and caddisflies (Shah et al., 2017) show wider thermal breadths than their lowland counterparts. Whilst the underlying mechanisms need to be further explored, such a pattern may be associated with the broader range of climatic conditions in high-mountain areas, in agreement with the Climatic Variability Hypothesis (Stevens, 1989), which predicts a positive relationship between species thermal tolerance and the degree of climatic variability they experience. It has also been suggested that the higher heat tolerance of alpine species could be an indirect consequence of adaptation to high UV radiation in these habitats (Sommaruga, 2001), through changes in the cuticle structure or thickness related to radiation management, which could indirectly increase heat tolerance trough passive thermoregulation (Alves et al., 2018; Carbonell et al., 2024).

At the intra-lineage level, *A. bipustulatus* showed significant variation in thermal limits amongst populations, but previous work has found no evidence that such intraspecific variation could be related to local adaptation to different thermal conditions along altitudinal gradients (Pallarés et al., 2024). Therefore, our results suggest that, as with body shape, local adaptation has driven changes in thermal tolerance traits in the micro-endemic *A. nevadensis*, but parallel evolution across altitudinal gradients has not taken place in its sister Iberian lineage of *A. bipustulatus* (Pallarés et al., 2024). It should be noted that the differences in thermal limits within and between lineages, though significant, were very small in magnitude (generally <1°C). Whilst our laboratory approach employing fast ramping rates does not mimic what happens in the field, it provides a sound comparative framework for understanding relative thermal tolerance of taxa and populations. Further research would clearly be needed to elucidate the specific mechanisms underlying heat tolerance in the study species. Despite this, the different capacities to deal with heat stress observed here are likely to be relevant in a climate warming context. Recent research demonstrates that in aquatic environments, both water temperature and oxygen availability may modulate organismal responses to climate change, by altering their aerobic metabolism (Rubalcaba et al., 2020). Warmer water temperatures increase oxygen demand relative to supply, reducing aerobic scope and hence the energy budgets needed to support the activities of aquatic animals.

The *Agabus bipustulatus* complex represents an interesting and intricate case of morphological and physiological differentiation with altitude in temperate mountain systems. Some traits appear to be subject to parallel altitudinal adaptive selection across the Palearctic (Drotz et al., 2001; Drotz et al., 2012) whilst, within an Iberian context, populations in the Sierra Nevada appear to have followed a unique evolutionary path. These findings may inspire further research aimed at elucidating the specific selective forces shaping morphological and physiological variation along elevation gradients in this species complex.

4.3 | Taxonomic and conservation implications

Although taxonomic uncertainty is often problematic in the context of conservation planning, it is widely recognised that conservation strategies should aim to maximise evolutionary potential (Stanton et al., 2019). This is where integrative taxonomy approaches are useful to identify taxa or populations of potential conservation interest, due to their genetic and ecological uniqueness. Under such framework, we shed light into the evolutionary history of a species complex that has been the subject of taxonomic debate for more than a century, providing significant insights into the processes that shape phenotypic and genetic diversity in isolated alpine ecosystems, themselves of great conservation concern.

Our results suggest that *A. nevadensis* is an alpine 'ecotype' of *A. bipustulatus*, resulting from an interplay between local adaptation and geographical isolation fuelled by Pleistocene glacial cycles. The coexistence of both lineages in multiple localities – often forming hybrid swarms – suggests that the incipient speciation of *A. nevadensis* could be reversed by hybridisation with its more widespread sister lineage. Furthermore, a recent study predicted an almost complete loss of the climatically suitable area for *A. nevadensis* in a warming climate (Pallarés et al., 2020), drawing attention to its vulnerability to climate change. If conserving adaptive potential is a priority, there is no doubt that *A. nevadensis* deserves attention from a conservation perspective. Our analyses also point, for the first time, to incipient speciation involving Iberian and trans-Palearctic populations of *A. bipustulatus*, suggesting that we need a reappraisal of the taxonomy of the whole complex, with a special focus on the many alpine forms that have been described (Nilsson & Hájek, 2021). Future studies assessing hybrid viability and fitness, exploring other morphological and physiological traits associated with alpine adaptation, such as desiccation resistance, tolerance to hypoxia and UV radiation or flight capacity, across a wider range of populations, or applying functional niche approaches to determine the degree of niche differentiation between lineages, could shed light on the relative role of ecological and geographical factors in driving lineage divergence. In short, this species complex has the potential to help us address a number of outstanding questions in alpine ecology and evolution.

AUTHOR CONTRIBUTIONS

Designed research: PA, SP, JO; field sampling: PA, SP, DTB, JAC, AM; genomic library preparation: EF-F, JO; performed morphometric measurements: EF-F, JAC, SP; performed thermal tolerance experiments: SP, JAC; analysed data: SP, JO; wrote first draft: SP; revised the manuscript: all authors.

ACKNOWLEDGEMENTS

This work was supported by the R&D project id. PID2019-108895GB-I00, funded by MCIN/AEI/ 10.13039/501100011033 and VI PPIT Universidad de Sevilla (IV.7 Ayuda Suplementaria a Grupos de Investigación por captación de fondos en las convocatorias de proyectos de investigación del Plan Estatal; 2020/1110). Logistic support was provided by Laboratorio de Ecología Molecular (LEM-EBD) from Estación Biológica de Doñana (CSIC). We also thank Centro de Supercomputación de Galicia (CESGA) and Doñana's Singular Scientific-Technical Infrastructure (ICTS-RBD) for access to computer resources. SP is funded by a postdoctoral contract from the 'Consejería de Economía, Conocimiento, Empresas y Universidad de la Junta de Andalucía-Fondo Social Europeo de Andalucía 2014-2020' ('Talento Doctores, PID 2020' program, grant id. SP-DOC_01211). JAC is funded by a postdoctoral contract from the 'María Zambrano' program (grant id. 19868), by the Spanish 'Ministerio de Universidades' (funded by European Union – NextGenerationEU). The Sierra Nevada National Park authorities and Andalusian Government provided logistic help and sampling permissions. We are especially grateful to Félix Picazo, David Sánchez-Fernández and Narcisa Martínez for help at various stages of this project. DTB thanks Rebecca Bilton, Shidi and Fara Hosseinie, Hiva Nasserzadeh, Michael Balke, Mario Toledo, Antonio Schizzerotto and Steven Routledge for their help in the field. We thank three anonymous referees for their constructive and valuable comments on an earlier version of the manuscript.

CONFLICT OF INTEREST STATEMENT

The authors have no conflicts of interest to declare.

DATA AVAILABILITY STATEMENT

Raw Illumina reads have been deposited at the NCBI Sequence Read Archive (SRA) under BioProject PRJNA1111346. Datasets and input files for all genomic analyses (STRUCTURE, NEWHYBRIDS, SVDQUARTETS, STAIRWAY PLOT and FASTSIMCOAL2), geometric morphometry analyses (generalised Procrustes analyses and Procrustes ANOVA) and thermal tolerance analyses (GLMs) are available for download on Figshare (https://doi.org/10.6084/m9.figshare.25858969).

BENEFIT-SHARING STATEMENT

A research collaboration network was developed with scientists from the institutions and countries providing samples, all collaborators are included as co-authors, the results of research have been shared with the broader scientific community and general audience, and the research addresses a priority concern, in this case the conservation of the organisms being studied. Benefits from this research also accrue from the sharing of our data and results on public databases as described above.

ORCID

Susana Pallarés https://orcid.org/0000-0001-8677-7475
Joaquín Ortego https://orcid.org/0000-0003-2709-429X

REFERENCES

Abellán, P., & Svenning, J. C. (2014). Refugia within refugia–patterns in endemism and genetic divergence are linked to late quaternary climate stability in the Iberian Peninsula. *Biological Journal of the Linnean Society*, *113*, 13–28.

Adams, D. C., & Otarola-Castillo, E. (2013). *Geomorph*: An R package for the collection and analysis of geometric morphometric shape data. *Methods in Ecology and Evolution*, *4*, 393–399.

Alves, P. C., Melo-Ferreira, J., Frieyas, H., & Boursot, P. (2008). The ubiquitous mountain hare mitochondria: Multiple introgressive hybridization in hares, genus *Lepus*. *Philosophical Transactions of the Royal Society B: Biological Sciences*, *363*, 2831–2839.

Alves, V. M., Hernandez, M. I., & Lobo, J. M. (2018). Elytra absorb ultraviolet radiation but transmit infrared radiation in Neotropical *Canthon* species (Coleoptera, Scarabaeinae). *Photochemistry and Photobiology*, *94*, 532–539.

Anderson, E. C., & Thompson, E. A. (2002). A model-based method for identifying species hybrids using multilocus genetic data. *Genetics*, *160*, 1217–1229.

Anderson, M. J., & Ter Braak, C. J. F. (2003). Permutation tests for multifactorial analysis of variance. *Journal of Statistical Computation and Simulation*, *73*, 85–113.

Angus, R. B., Clery, M. J., Carter, J. C., & Wenczek, D. E. (2013). Karyotypes of some medium-sized Dytiscidae (Agabinae and Colymbetinae) (Coleoptera). *Comparative Cytogenetics*, *7*, 171–190.

Antonelli, A., Kissling, W. D., Flantua, S. G., Bermúdez, M. A., Mulch, A., Muellner-Riehl, A. N., Kreft, H., Linder, H. P., Badgley, C., Fjeldså, J., Fritz, S. A., Rahbek, C., Herman, F., Hooghiemstra, H., & Hoorn, C. (2018). Geological and climatic influences on mountain biodiversity. *Nature Geoscience*, *11*, 718–725.

Arribas, P., Velasco, J., Abellán, P., Sánchez-Fernández, D., Andújar, C., Calosi, P., Millán, A., Ribera, I., & Bilton, D. T. (2012). Dispersal ability rather than ecological tolerance drives differences in range size between lentic and lotic water beetles (Coleoptera: Hydrophilidae). *Journal of Biogeography*, *39*, 984–994.

Arroyo, J., Abellán, P., Arista, M., Ariza, M. J., de Castro, A., Escudero, M., Lorite, J., Martínez-Borda, E., Mejías, J. A., Molina-Venegas, R., Pleguezuelos, J. M., Simón-Porcar, V., & Viruel, J. (2022). Sierra Nevada, a Mediterranean biodiversity super hotspot. In R. Zamora & M. Oliva (Eds.), *The landscape of the Sierra Nevada: A unique Laboratory of Global Processes in Spain* (pp. 11–30). Springer International Publishing.

Avise, J. C. (2000). *Phylogeography: The history and formation of species*. Harvard University Press.

Baker, A. J. (2008). Islands in the sky: The impact of Pleistocene climate cycles on biodiversity. *Journal of Biology*, *7*, 32.

Balfour-Browne, W. A. F. (1950). *British water beetles* (Vol. *2*). Ray Society.

Behm, J. E., Ives, A. R., & Boughman, J. W. (2010). Breakdown in postmating isolation and the collapse of a species pair through hybridization. *American Naturalist*, *175*, 11–26.

Bennett, K. D., & Provan, J. (2008). What do we mean by 'refugia'? *Quaternary Science Reviews*, *27*, 2449–2455.

Bergsten, J., Bilton, D. T., Fujisawa, T., Elliott, M., Monaghan, M. T., Balke, M., Hendrich, L., Geijer, J., Herrmann, J., Foster, G. N., Ribera, I., Nilsson, A. N., Barraclough, T. G., & Vogler, A. P. (2012). The effect of geographical scale of sampling on DNA barcoding. *Systematic Biology*, *61*, 851–869.

Bertola, L. D., Quinn, L., Hanghøj, K., Garcia-Erill, G., Rasmussen, M. S., Balboa, R. F., Meisner, J., Bøggild, T., Wang, X., Lin, L., Nursyifa, C., Liu, X., Li, Z., Chege, M., Moodley, Y., Brüniche-Olsen, A., Kuja, J., Schubert, M., Agaba, M., … Heller, R. (2024). Giraffe lineages are shaped by major ancient admixture events. *Current Biology*, *34*, 1576–1586.

Butlin, R. (1987). Speciation by reinforcement. *Trends in Ecology & Evolution*, *2*, 8–13.

Calosi, P., Bilton, D. T., Spicer, J. I., Votier, S. C., & Atfield, A. (2010). What determines a species' geographical range? Thermal biology and latitudinal range size relationships in European diving beetles (Coleoptera: Dytiscidae). *Journal of Animal Ecology*, *79*, 194–204.

Carbonell, J. A., Pallarés, S., Velasco, J., Millán, A., & Abellán, P. (2024). Thermal tolerance does not explain the altitudinal segregation of lowland and alpine aquatic insects. *Journal of Thermal Biology*, *121*, 103862.

Catchen, J., Hohenlohe, P. A., Bassham, S., Amores, A., & Cresko, W. A. (2013). STACKS: An analysis tool set for population genomics. *Molecular Ecology*, *22*(11), 3124–3140.

Chen, G., & Hare, M. (2008). Cryptic ecological diversification of a planktonic estuarine copepod, *Acartia tonsa*. *Molecular Ecology*, *17*, 1451–1468.

Chifman, J., & Kubatko, L. (2014). Quartet inference from SNP data under the coalescent model. *Bioinformatics*, *30*(23), 3317–3324.

Chown, S. L., & Terblanche, J. S. (2006). Physiological diversity in insects: Ecological and evolutionary contexts. *Advances in Insect Physiology*, *33*, 50–152.

Čiamporová-Zaovičová, Z., & Čiampor, F. (2011). Aquatic beetles of the alpine lakes: Diversity, ecology and small-scale population genetics. *Knowledge and Management of Aquatic Ecosystems*, *402*, 10.

Coates, D. J., Byrne, M., & Moritz, C. (2018). Genetic diversity and conservation units: Dealing with the species-population continuum in the age of genomics. *Frontiers in Ecology and Evolution*, *6*, 165.

Collyer, M. L., Sekora, D. J., & Adams, D. C. (2015). A method for analysis of phenotypic change for phenotypes described by high-dimensional data. *Heredity*, *115*, 357–365.

Degerlund, M., Huseby, S., Zingone, A., Sarno, D., & Landfald, B. (2012). Functional diversity in cryptic species of *Chaetoceros socialis* Lauder (Bacillariophyceae). *Journal of Plankton Research*, *34*, 416–431.

Drotz, M. K., Brodin, T., & Nilsson, A. N. (2010). Multiple origins of elytral reticulation modifications in the west Palearctic *Agabus bipustulatus* complex (Coleoptera, Dytiscidae). *PLoS One*, *5*, e9034.

Drotz, M. K., Brodin, T., Saura, A., & Giles, B. E. (2012). Ecotype differentiation in the face of gene flow within the diving beetle *Agabus bipustulatus* (Linnaeus, 1767) in northern Scandinavia. *PLoS One*, *7*, e31381.

Drotz, M. K., Saura, A., & Nilsson, A. N. (2001). The species delimitation problem applied to the *Agabus bipustulatus* complex (Coleoptera, Dytiscidae) in north Scandinavia. *Biological Journal of the Linnean Society*, *73*, 11–22.

Dynesius, M., & Jansson, R. (2000). Evolutionary consequences of changes in species' geographical distributions driven by Milankovitch climate oscillations. *Proceedings of the National Academy of Sciences United States of America*, *97*, 9115–9120.

Dynesius, M., & Jansson, R. (2014). Persistence of within-species lineages: A neglected control of speciation rates. *Evolution*, *68*, 923–934.

Earl, D. A., & vonHoldt, B. M. (2012). STRUCTURE HARVESTER: A website and program for visualizing structure output and implementing the Evanno method. *Conservation Genetics Resources*, *4*(2), 359–361.

Evanno, G., Regnaut, S., & Goudet, J. (2005). Detecting the number of clusters of individuals using the software v: A simulation study. *Molecular Ecology*, *14*(8), 2611–2620.

Excoffier, L., Dupanloup, I., Huerta-Sanchez, E., Sousa, V. C., & Foll, M. (2013). Robust demographic inference from genomic and SNP data. *PLoS Genetics*, *9*(10), e1003905.

Excoffier, L., & Lischer, H. E. (2010). ARLEQUIN suite ver 3.5: A new series of programs to perform population genetics analyses under Linux and Windows. *Molecular Ecology Resources*, *10*(3), 564–567.

Fick, S. E., & Hijmans, R. J. (2017). WorldClim 2: New 1km spatial resolution climate surfaces for global land areas. *International Journal of Climatology*, *37*, 4302–4315.

Flantua, S. G., Payne, D., Borregaard, M. K., Beierkuhnlein, C., Steinbauer, M. J., Dullinger, S., Essl, F., Irl, S. D. H., Kienle, D., Kreft, H., Lenzner, B., Norder, S. J., Rijsdijk, K. F., Rumpf, S. B., Weigelt, P., & Field, R. (2020). Snapshot isolation and isolation history challenge the analogy between mountains and islands used to understand endemism. *Global Ecology and Biogeography*, *29*, 1651–1673.

Galewski, K., & Tranda, E. (1978). *Fauna Słodkowodna Polski, Chrz szcze (Coleoptera), Rodziny Pływakowate (Dytiscidae), Fliskowate*

(Haliplidae), Mokrzelicowate (Hygrobiidae), Kretakowate (Gyrinidae) (p. 396). PWN.

García-Vázquez, D., Bilton, D. T., Foster, G. N., & Ribera, I. (2017). Pleistocene range shifts, refugia and the origin of widespread species in western Palaearctic water beetles. *Molecular Phylogenetics and Evolution*, *114*, 122–136.

Garrick, R. C., Benavides, E., Russello, M. A., Hyseni, C., Edwards, D. L., Gibbs, J. P., Tapia, W., Ciofi, C., & Caccone, A. (2014). Lineage fusion in Galápagos giant tortoises. *Molecular Ecology*, *23*, 5276–5290.

Gonzalez, V. H., Oyen, K., Vitale, N., & Ospina, R. (2022). Neotropical stingless bees display a strong response in cold tolerance with changes in elevation. *Conservation Physiology*, *10*, coac073.

Gómez, A., & Lunt, D. H. (2007). Refugia within refugia: Patterns of phylogeographic concordance in the Iberian Peninsula. In S. Weiss & N. Ferrand (Eds.), *Phylogeography of southern European Refugia: Evolutionary perspectives on the origins and conservation of European biodiversity* (pp. 155–188). Springer.

Gómez-Ortiz, A., Oliva, M., Salvà-Catarineu, M., & Salvador-Franch, F. (2013). The environmental protection of landscapes in the high semiarid Mediterranean mountain of Sierra Nevada National Park (Spain): Historical evolution and future perspectives. *Applied Geography*, *42*, 227–239.

Goodall, C. R. (1991). Procrustes methods in the statistical analysis of shape. *Journal of the Royal Statistical Society Series B*, *53*, 285–339.

Gruber, B., Unmack, P. J., Berry, O. F., & Georges, A. (2018). *dartR*: An R package to facilitate analysis of SNP data generated from reduced representation genome sequencing. *Molecular Ecology Resources*, *18*(3), 691–699.

Hedin, M., Carlson, D., & Coyle, F. (2015). Sky Island diversification meets the multispecies coalescent–divergence in the spruce-fir moss spider (*Microhexura montivaga*, Araneae, Mygalomorphae) on the highest peaks of southern Appalachia. *Molecular Ecology*, *24*, 3467–3484.

Hedrick, P. W. (2013). Adaptive introgression in animals: Examples and comparison to new mutation and standing variation as sources of adaptive variation. *Molecular Ecology*, *22*, 4606–4618.

Hewitt, G. (2000). The genetic legacy of the quaternary ice ages. *Nature*, *405*, 907–913.

Hewitt, G. M. (1999). Post-glacial re-colonization of European biota. *Biological Journal of the Linnean Society*, *68*(1–2), 87–112.

Jakobsson, M., & Rosenberg, N. A. (2007). CLUMPP: A cluster matching and permutation program for dealing with label switching and multimodality in analysis of population structure. *Bioinformatics*, *23*(14), 1801–1806.

Jombart, T. (2008). *Adegenet*: A R package for the multivariate analysis of genetic markers. *Bioinformatics*, *24*(11), 1403–1405.

Kearns, A. M., Restani, M., Szabo, I., Schrøder-Nielsen, A., Kim, J. A., Richardson, H. M., Marzluff, J. M., Fleischer, R. C., Johnsen, A., & Omland, K. E. (2018). Genomic evidence of speciation reversal in ravens. *Nature Communications*, *9*, 906.

Keightley, P. D., Ness, R. W., Halligan, D. L., & Haddrill, P. R. (2014). Estimation of the spontaneous mutation rate per nucleotide site in a *Drosophila melanogaster* full-sib family. *Genetics*, *196*(1), 313–320.

Keller, I., Alexander, J. M., Holderegger, R., & Edwards, P. J. (2013). Widespread phenotypic and genetic divergence along altitudinal gradients in animals. *Journal of Evolutionary Biology*, *26*, 2527–2543.

Kleindorfer, S., O'Connor, J. A., Dudaniec, R. Y., Myers, S. A., Robertson, J., & Sulloway, F. J. (2014). Species collapse via hybridization in Darwin's tree finches. *The American Naturalist*, *183*, 325–341.

Klingenberg, C. P. (2011). MorphoJ: An integrated software package for geometric morphometrics. *Molecular Ecology Resources*, *11*, 353–357.

Körner, C. (2007). The use of 'altitude' in ecological research. *Trends in Ecology and Evolution*, *22*, 569–574.

Liu, X. M., & Fu, Y. X. (2020). Stairway Plot 2: Demographic history inference with folded SNP frequency spectra. *Genome Biology*, *21*(1), 280.

Love, S. J., Schweitzer, J. A., Woolbright, S. A., & Bailey, J. K. (2023). Sky islands are a global tool for predicting the ecological and evolutionary consequences of climate change. *Annual Review of Ecology, Evolution, and Systematics*, *54*, 219–236.

Lukicheva, S., & Mardulyn, P. (2021). Whole-genome sequencing reveals asymmetric introgression between two sister species of cold-resistant leaf beetles. *Molecular Eecology*, *30*, 4077–4089.

Lutterschmidt, W. I., & Hutchison, V. H. (1997). The critical thermal maximum: History and critique. *Canadian Journal of Zoology*, *75*, 1561–1574.

Maier, P. A., Vandergast, A. G., Ostoja, S. M., Aguilar, A., & Bohonak, A. J. (2019). Pleistocene glacial cycles drove lineage diversification and fusion in the Yosemite toad (*Anaxyrus canorus*). *Evolution*, *73*, 2476–2496.

Mavárez, J., & Linares, M. (2008). Homoploid hybrid speciation in animals. *Molecular Ecology*, *17*, 4181–4185.

McCulloch, G. A., Foster, B. J., Dutoit, L., Ingram, T., Hay, E., Veale, A. J., Dearden, P. K., & Waters, J. M. (2019). Ecological gradients drive insect wing loss and speciation: The role of the alpine treeline. *Molecular Ecology*, *28*, 3141–3150.

Médail, F., & Quézel, P. (1997). Hot-spots analysis for conservation of plant biodiversity in the Mediterranean Basin. *Annals of the Missouri Botanical Garden*, *84*, 112–127.

Médail, F., & Quézel, P. (1999). Biodiversity hotspots in the Mediterranean Basin: Setting global conservation priorities. *Conservation Biology*, *13*, 1510–1513.

Millán, A., Picazo, F., Sánchez-Fernández, D., Abellán, P., & Ribera, I. (2013). Los Coleópteros acuáticos amenazados (Coleoptera). In F. Ruano, M. Tierno de Figueroa, & A. Tinaut (Eds.), *Los Insectos de Sierra Nevada. 200 años de historia* (pp. 443–456). Asociación Española de Entomología.

Millán, A., Sánchez-Fernández, D., Abellán, P., Picazo, F., Carbonell, J. A., Lobo, J. M., & Ribera, I. (2014). *Atlas de los coleópteros acuáticos de España peninsular*. Ministerio de Agricultura, Alimentación y Medio Ambiente.

Miller, K. B., & Bergsten, J. (2016). *Diving beetles of the world: Systematics and biology of the Dytiscidae*. JHU Press.

Momigliano, P., Florin, A. B., & Merilä, J. (2021). Biases in demographic modeling affect our understanding of recent divergence. *Molecular Biology and Evolution*, *38*(7), 2967–2985.

Muangmai, N., Preuss, M., & Zuccarello, G. C. (2015). Comparative physiological studies on the growth of cryptic species of *Bostrychia intricata* (Rhodomelaceae, Rhodophyta) in various salinity and temperature conditions. *Phycological Research*, *63*, 300–306.

Múrria, C., Sáinz-Bariáin, M., Vogler, A. P., Viza, A., González, M., & Zamora-Muñoz, C. (2020). Vulnerability to climate change for two endemic high-elevation, low-dispersive Annitella species (Trichoptera) in Sierra Nevada, the southernmost high mountain in Europe. *Insect Conservation and Diversity*, *13*, 283–295.

Nilsson, A. N., & Hájek, J. (2021). *A World Catalogue of the Family Dytiscidae, or the Diving Beetles (Coleoptera, Adephaga). Version 1.I.2021*. http://www.waterbeetles.eu

Nilsson, A. N., & Holmen, M. (1995). The aquatic Adephaga (Coleoptera) of Fennoscandia and Denmark. II. Dytiscidae. *Fauna Entomologica Scandinavica*, *32*, 1–192.

Nilsson, A. N., & Persson, S. (1990). Dimorphism of the metasternal wing in *Agabus raffrayi* and *A. labiatus* (Coleoptera: Dytiscidae) questioned. *Aquatic Insects*, *12*, 135–144.

Noguerales, V., Arjona, Y., García-Olivares, V., Machado, A., López, H., Patiño, J., & Emerson, B. C. (2024). Genetic legacies of megalandslides: Cycles of isolation and contact across flank collapses in an oceanic Island. *Molecular Ecology*, *33*(9), e17341.

Noguerales, V., & Ortego, J. (2022). Genomic evidence of speciation by fusion in a recent radiation of grasshoppers. *Evolution*, *76*, 2618–2633.

Ortego, J., Gutiérrez-Rodríguez, J., & Noguerales, V. (2021). Demographic consequences of dispersal-related trait shift in two recently diverged taxa of montane grasshoppers. *Evolution*, *75*, 1998–2013.

Ortego, J., & Knowles, L. L. (2022). Geographical isolation versus dispersal: Relictual alpine grasshoppers support a model of interglacial diversification with limited hybridization. *Molecular Ecology*, *31*, 296–312.

Pallarés, S., Carbonell, J. A., Picazo, F., Bilton, D. T., Millán, A., & Abellán, P. (2024). Intraspecific variation of thermal tolerance in freshwater insects along elevational gradients: The case of a widespread diving beetle. *bioRxiv*. https://doi.org/10.1101/2024.03.04.583263

Pallarés, S., Millán, A., Mirón, J. M., Velasco, J., Sánchez-Fernández, D., Botella-Cruz, M., & Abellán, P. (2020). Assessing the capacity of endemic alpine water beetles to face climate change. *Insect Conservation and Diversity*, *13*, 271–282.

Peterson, B. K., Weber, J. N., Kay, E. H., Fisher, H. S., & Hoekstra, H. E. (2012). Double digest RADseq: An inexpensive method for de novo SNP discovery and genotyping in model and non-model species. *PLoS One*, *7*(5), e37135.

Pritchard, J. K., Stephens, M., & Donnelly, P. (2000). Inference of population structure using multilocus genotype data. *Genetics*, *155*(2), 945–959.

R Core Team. (2021). *R: A language and environment for statistical computing*. R Foundation for Statistical Computing. https://www.R-project.org/

Ribera, I., Castro, A., Díaz, J. A., Garrido, J., Izquierdo, A., Jäch, M. A., & Valladares, L. F. (2011). The geography of speciation in narrow-range endemics of the 'Haenydra' lineage (Coleoptera, Hydraenidae, Hydraena). *Journal of Biogeography*, *38*, 502–516.

Ribera, I., Foster, G. N., & Holt, W. V. (1997). Functional types of diving beetle (Coleoptera: Hygrobiidae and Dytiscidae), as identified by comparative swimming behaviour. *Biological Journal of Linnaean Society*, *61*, 537–558.

Ribera, I., Hernando, C., & Aguilera, P. (1998). An annotated checklist of the Iberian water beetles (Coleoptera). *Zapateri*, *8*, 43–111.

Ribera, I., & Nilsson, A. (1995). Morphometric patterns among diving beetles (Coleoptera: Noteridae, Hygrobiidae, and Dytiscidae). *Canadian Journal of Zoology*, *73*, 2343–2360.

Ribera, I., & Vogler, A. P. (2004). Speciation of Iberian diving beetles in Pleistocene refugia (Coleoptera, Dytiscidae). *Molecular Ecology*, *13*, 179–193.

Rohlf, F. J. (2015). The TPS series of software. *Hystrix-Italian Journal of Mammalogy*, *26*, 9–12.

Rosenberg, N. A. (2004). Distruct: A program for the graphical display of population structure. *Molecular Ecology Notes*, *4*(1), 137–138.

Ruano, F., Tierno de Figueroa, J., & Tinaut, A. (2013). *Los insectos de Sierra Nevada: 2000 años de historia*. Asociación Española de Entomología.

Rubalcaba, J. G., Verberk, W. C., Hendriks, A. J., Saris, B., & Woods, H. A. (2020). Oxygen limitation may affect the temperature and size dependence of metabolism in aquatic ectotherms. *Proceedings of the National Academy of Sciences*, *117*(50), 31963–31968.

Schmitt, T. (2007). Molecular biogeography of Europe: Pleistocene cycles and postglacial trends. *Frontiers in Zoology*, *4*, 11.

Schoville, S. D., Roderick, G. K., & Kavanaugh, D. H. (2012). Testing the 'Pleistocene species pump'in alpine habitats: Lineage diversification of flightless ground beetles (Coleoptera: Carabidae: Nebria) in relation to altitudinal zonation. *Biological Journal of the Linnean Society*, *107*, 95–111.

Seehausen, O. (2006). Conservation: Losing biodiversity by reverse speciation. *Current Biology*, *16*, R334–R337.

Seehausen, O., Takimoto, G., Roy, D., & Jokela, J. (2008). Speciation reversal and biodiversity dynamics with hybridization in changing environments. *Molecular Ecology*, *17*, 30–44.

Shah, A. A., Gill, B. A., Encalada, A. C., Flecker, A. S., Funk, W. C., Guayasamin, J. M., Kondratieff, B. C., Poff, N. L. R., Thomas, S. A., Zamudio, K. R., & Ghalambor, C. K. (2017). Climate variability predicts thermal limits of aquatic insects across elevation and latitude. *Functional Ecology*, *31*(11), 2118–2127.

Sharp, D. (1882). On aquatic carnivorous Coleoptera or Dytiscidae. *The Scientific transactions of the Royal Dublin Society, Series 2*, *2*, 17–1003.

Slatyer, R. A., & Schoville, S. D. (2016). Physiological limits along an elevational gradient in a radiation of montane ground beetles. *PLoS One*, *11*. e0151959.

Sommaruga, R. (2001). The role of solar UV radiation in the ecology of alpine lakes. *Journal of Photochemistry and Photobiology B: Biology*, *62*(1–2), 35–42.

Stanbrook, R., Wheater, C. P., Harris, W. E., & Jones, M. (2021). Habitat type and altitude work in tandem to drive the community structure of dung beetles in Afromontane forest. *Journal of Insect Conservation*, *25*, 159–173.

Stanton, D. W., Frandsen, P., Waples, R. K., Heller, R., Russo, I. R. M., Orozco-terWengel, P. A., Tingskov Pedersen, C.-E., Siegismund, H. R., & Bruford, M. W. (2019). More grist for the mill? Species delimitation in the genomic era and its implications for conservation. *Conservation Genetics*, *20*, 101–113.

Steinbauer, M. J., Irl, S. D. H., & Beierkuhnlein, C. (2013). Elevation driven ecological isolation promotes-diversification on Mediterranean islands. *Acta Oecologica*, *47*, 52–56.

Stevens, G. C. (1989). The latitudinal gradient in geographical range: How so many species coexist in the tropics. *The American Naturalist*, *133*, 240–256.

Stewart, J. R., Lister, A. M., Barnes, I., & Dalen, L. (2010). Refugia revisited: Individualistic responses in space and time. *Proceedings of the Royal Society B: Biological Sciences*, *277*, 661–671.

Swofford, D. L. (2002). *PAUP*. Phylogenetic analysis using parsimony (*and other methods). Version 4*. Sinauer Associates.

Taylor, E. B., Boughman, J. W., Groenenboom, M., Sniatynski, M., Schluter, D., & Gow, J. L. (2006). Speciation in reverse: Morphological and genetic evidence of the collapse of a three-spined stickleback (*Gasterosteus aculeatus*) species pair. *Molecular Ecology*, *15*, 343–355.

Tonzo, V., & Ortego, J. (2021). Glacial connectivity and current population fragmentation in sky islands explain the contemporary distribution of genomic variation in two narrow-endemic montane grasshoppers from a biodiversity hotspot. *Diversity and Distributions*, *27*, 1619–1633.

Tonzo, V., Papadopoulou, A., & Ortego, J. (2019). Genomic data reveal deep genetic structure but no support for current taxonomic designation in a grasshopper species complex. *Molecular Ecology*, *28*, 3869–3886.

Tribsch, A. (2004). Areas of endemism of vascular plants in the eastern Alps in relation to Pleistocene glaciation. *Journal of Biogeography*, *31*, 747–760.

Tsuchiya, Y., Takami, Y., Okuzaki, Y., & Sota, T. (2012). Genetic differences and phenotypic plasticity in body size between high-and low-altitude populations of the ground beetle *Carabus tosanus*. *Journal of Evolutionary Biology*, *25*, 1835–1842.

Vonlanthen, P., Bittner, D., Hudson, A. G., Young, K. A., Müller, R., Lundsgaard-Hansen, B., Roy, D., Di Piazza, S., Largiader, C. R., & Seehausen, O. (2012). Eutrophication causes speciation reversal in whitefish adaptive radiations. *Nature*, *482*, 357–362.

Webb, W. C., Marzluff, J. M., & Omland, K. E. (2011). Random interbreeding between cryptic lineages of the common raven: Evidence for speciation in reverse. *Molecular Ecology*, *20*, 2390–2402.

Weir, B. S., & Cockerham, C. C. (1984). Estimating F-statistics for the analysis of population structure. *Evolution*, *38*, 1358–1370.

Weir, J. T., & Schluter, D. (2004). Ice sheets promote speciation in boreal birds. *Proceedings of the Royal Society B: Biological Sciences*, *271*, 1881–1887.

Zamora, R., & Oliva, M. (Eds.). (2022). *The landscape of the Sierra Nevada: A unique Laboratory of Global Processes in Spain*. Springer Nature.
Zelditch, M. L., Swiderski, D. L., Sheets, H. D., & Fink, W. L. (2004). *Geometric morphometrics for biologists: A primer*. Elsevier Academic Press.

SUPPORTING INFORMATION

Additional supporting information can be found online in the Supporting Information section at the end of this article.

How to cite this article: Pallarés, S., Ortego, J., Carbonell, J. A., Franco-Fuentes, E., Bilton, D. T., Millán, A., & Abellán, P. (2024). Genomic, morphological and physiological data support fast ecotypic differentiation and incipient speciation in an alpine diving beetle. *Molecular Ecology*, *33*, e17487. https://doi.org/10.1111/mec.17487